Efficient Access Control for Power Line Communication Networks

by

Yinjia Huo

B.A.Sc., Zhejiang University, 2014

A THESIS SUBMITTED IN PARTIAL FULFILLMENT
OF THE REQUIREMENTS FOR THE DEGREE OF

Master of Applied Science

in

THE FACULTY OF GRADUATE AND POSTDOCTORAL STUDIES
(Electrical and Computer Engineering)

The University of British Columbia
(Vancouver)

April 2017

Abstract

Broadband power line communications (BB-PLC) reuse power line infrastructure to provide high-speed and high-penetration data transmissions, which make BB-PLC an attractive solution to in-vehicle networks (IVNs) and home area networks (HANs). However, there still exist many research issues that need to be addressed before we can readily apply BB-PLC to these two application scenarios. To partially address these issues, the thesis proposes some efficient access control schemes by extending a popular BB-PLC protocol, HomePlug AV (HPAV).

The latency performance of the original HPAV protocol is not satisfactory for IVNs. Thus, we introduce the Virtual Collision (VC) mechanism as an enhancement to the HPAV random back-off procedure to reduce the queuing latency. In addition, the relationships between transmissions of different classes of network traffic involved in an IVN are not well handled by the strict priority transmission selection algorithm (TXSA) specified in the HPAV protocol. In this regard, we propose to combine the strict priority TXSA with the Audio Video Bridging credit-based shaping (CBS) TXSA.

The efficiency of the HPAV medium access control (MAC) layer is restricted by various MAC overheads, which makes the deployment of BB-PLC in a HAN less attractive. We use the emerging in-band full duplexing capability to enable two new techniques, Mutual Preamble Detection (MPD) and Contention Free Pre-sensing (CFP) to reduce these overheads. Then, aiming to provide a unified solution to support various HAN applications, we develop an interface with prioritization and traffic shaping to accommodate the heterogeneous network traffic involved.

We use OMNeT++, a discrete event simulator, to verify the effectiveness of our proposed

schemes, by comparing the network performance with our proposed schemes to that of the original HPAV protocol. The simulation results show that VC satisfactorily reduces queuing latency, the new TXSA better handles different priorities, MPD works well with CFP to improve MAC efficiency and the developed interface functions properly.

While there still exist many research issues before we can exploit the full advantages of BB-PLC, our proposed schemes bring us one step closer towards that goal.

Preface

The efficient access control schemes developed for in-vehicle network in Chapter 3 of this thesis are based on the work conducted in UBC Wireless Networks and Mobile Systems Laboratory with Qiang Zheng, Dr. Zhengguo Sheng and Professor Victor C.M. Leung. The work has been published in paper #1 listed below. As the first author of this paper, I initiated and conducted most of the research. I conducted background survey, contributed in research ideas, performed the analysis and carried out simulations. Qiang Zheng and Dr. Zhengguo Sheng contributed in research ideas and algorithm formulation. Professor Victor C.M. Leung helped in research directions and manuscript proof-reading.

The efficient access control schemes developed for home area network in Chapter 4 of this thesis are based on the work conducted in UBC Wireless Networks and Mobile Systems Laboratory with Gautham Prasad, Professor Lutz Lampe and Professor Victor C.M. Leung. The work has been published partially in paper #2. Remaining part of the work is included in paper #3, which has been submitted to a journal. As the first author of these papers, I initiated and conducted most of the research. I conducted background survey in related topics, contributed in research ideas, performed the analysis and carried out simulations. Gautham Prasad contributed in mathematical modelling, simulation schemes and manuscript preparation. Professor Lutz lampe and Professor Victor C.M. Leung helped in research directions and manuscript proof-reading.

1. Yinjia Huo, Qiang Zheng, Zhengguo Sheng and Victor C.M. Leung, "Queuing Enhancements for In-Vehicle Time-Sensitive Streams Using Power Line Communications", in Proceedings of IEEE International Conference on Communications in China (ICCC), Shenzhen,

China, November 2015.

2. Yinjia Huo, Gautham Prasad, Lutz Lampe and Victor C.M. Leung, "Mutual Preamble Detection for Full Duplex Broadband Power Line Communications", in Proceedings of IEEE Global Communications Conference, Washington D.C., USA, December 2016.

3. Yinjia Huo, Gautham Prasad, Lutz Lampe and Victor C.M. Leung, "Efficient Access Control for Broadband Power Line Communications in Home Area Network", submitted to a journal, 10 pages, double column, March 2017.

Table of Contents

List of Tables

List of Figures

List of Abbreviations

ACK/NACK Acknowledgment/Negative Acknowledgment

AV Audio and Video

AVB Audio Video Bridging

BB-PLC Broadband Power Line Communications

BC Back-off Counter

BPC Back-off Procedure Event Counter

CA Collision Avoidance

CBS Credit-Based Shaping

CCo Central Coordinator

CD Collision Detection

CFC Contention Free Condition

CFP Contention Free Pre-sensing

CIFS Contention Inter-Frame Space

CN Contention Notification

CSMA Carrier Sense Multiple Access

CW Contention Window

DC Deferral Counter

EC Echo Cancellation

ECU Electronic Control Unit

EIFS Extended Inter-Frame Space

FC Frame Control

FIFO First-in-First-out

HAN Home Area Network

HD Half-Duplex

HPAV HomePlug AV

HPGP HomePlug Green PHY

IBFD In-Band Full Duplexing

IC Ideal Centralized

IVN In-Vehicle Network

MAC Medium Access Control

MPD Mutual Preamble Detection

OFDM Orthogonal Frequency Division Multiplexing

OOK On-Off Keying

PHY Physical

PLC Power Line Communications

PRP Priority Resolution Period

PRS Priority Resolution Slot

PSD Power Spectral Density

PTS Poisson Traffic Shaping

QoS Quality of Service

RIFS Response Inter-Frame Space

RSI Residue Self-Interference

RTS/CTS Request-to-Send/Clear-to-Send

SACK Selective Acknowledgment

SI Self-Interference

SNR Signal-to-Noise-Ratio

SOF Start of Frame

SOI Signal-of-Interest

TC Transmit Counter

TXSA Transmission Selection Algorithm

VC Virtual Collision

VCS Virtual Carrier Sense

Notations

χ_i bit value of the i-th PRS

η MAC efficiency

$\eta_{\max}$ Optimum MAC efficiency

γ signal-to-noise-ratio

$\gamma_{\min}$ minimum signal-to-noise-ratio

κ bandwidth allocation control threshold

κ_k network resource consumed by priority k message

$\lambda_{n,k}$ event rate for n-th node priority k message

μ approximated MAC frame interval

$\mu_{n,k}$ average MAC frame intervals for n-th node priority k message

$\psi(c)$ sub-carrier specific phase angle

Φ_{R} power of received signal

$\Psi_{\mathrm{R}}(f)$ PSD of received signal at frequency f

Ψ_{RSI} the average RSI PSD after non-ideal SI cancellation

$\Psi_{\mathrm{T}}(f)$ PSD of transmit signal at frequency f

$\Psi_{\mathrm{T,max}}$ maximum transmit signal PSD

τ a defined ratio of two network parameters

b_0 decision threshold of non-coherent OOK normalized to root-mean-square noise

b_{opt} optimum decision threshold normalized to root-mean-square noise

f_c central frequency of an OFDM subcarrier

$\mathscr{C}$ set of OFDM subcarriers used for PRS and preamble transmission

CW contention window

$\mathsf{CW}_{\max}$ maximum contention window

E_b received bit energy

$\mathbb{E}[n_{BF}]$ expected number of back-off time slots

Δf width of an OFDM subcarrier

f_1 lower frequency of all OFDM subcarriers

f_2 upper frequency of all OFDM subcarriers

$|H_{\min}|^2$ flat minimum channel gain

$H(f)$ power line channel transfer function at frequency f

$I_n(\cdot)$ n-th-order modified Bessel function of the first kind

$\widetilde{j_n}$ the least significant priority resolution bit of value '1' of node n

j_n a certain priority resolution bit of node n

K total number of network nodes

ℓ number of a certain time sample

L total number of time samples

m supported maximum priority resolution bits

$\max(\cdot)$ maximum

MaxFL maximum time duration of data payload

N total number of active nodes

$\mathscr{N}$ set of active network nodes

n number of a certain node

N_0 average PSD of the cumulative noise at the receiver

$N_{0,\mathrm{FD}}$ effective IBFD noise floor at the receiver

n_{ACK} number of successfully acknowledged packets

N_{pkt} number of total packets transmitted

P average physical layer data rate

P_{DE} detection error rate

P_e overall network node error rate

P_{FA} false alarm rate

p_n priority level of network node n

p_{std} supported maximum priority level

P_{tot} normalized total error

$\mathcal{Q}(\cdot)$ first-order Marcum-Q function

r_i physical data rate of i-th data packet

S MAC throughput

s_1 PRS signal

s_2 preamble signal

SCINR signal to cancelled interference plus noise ratio after EC

SNR_{HD} SNR in half duplex mode

T total time duration

t_{CIFS} time duration of the contention inter-frame space

t_{EIFS} time duration of the extended inter-frame space

t_{FC} time duration of a frame control

t_{FL} time duration of data payload

t_{pd} time interval for PRS detection

t_{RIFS} time duration of response inter-frame space

t_{SLOT} time interval for a back-off time slot

t_i time duration of i-th data packet

t_{p} time duration of a preamble

T_{S} total simulation time

$\mathbb{Z}^+$ set of all positive integers

Acknowledgments

I would like to take this chance to thank all of those who have helped me and supported me during my research work.

I would like to thank Professor Victor C.M. Leung as my supervisor of my graduate study. He introduced me to a promising and interesting field of study. I would like to appreciate Dr. Zhengguo Sheng, whom I worked with during my first year of graduate study. I would also like to thank Professor Lutz Lampe, who helped me a lot in understanding the underlying technology.

I would like to thank my colleague Gautham Prasad, who helped me a lot with theoretical models and mathematical derivations. I would like to thank my colleague Yuanfang Chi, who has offered a lot of help with research methods. I would like to thank Qiang Zheng, Xuan Dong and Wei Tu for discussing research issues and sharing opinions. I would like to thank Roberto Antonioli, Morgan Roff and Jia Liu who helped with the construction of simulation platform.

I would like to thank my parents for their continuous support.

This work has been supported by the Natural Sciences and Engineering Research Council of Canada (NSERC) and AUTO 21, Canada's automotive research and development program.

Dedication

This thesis is dedicated to my beloved family.

Chapter 1

Introduction

1.1 Motivations and Objectives

This thesis studies broadband power line communications (BB-PLC) in two specific application scenarios, the in-vehicle network (IVN) [1] and the home area network (HAN) [2].

As a mature technology, PLC was first employed by utility companies for monitoring, controlling and maintaining the power grid [3]. Recent advances in signal processing techniques have enabled PLC to provide high-speed data communications through BB-PLC [4]. Among various applications of BB-PLC, two promising fields are IVN and HAN.

IVNs provide solutions to communications among various electronic control units (ECUs), sensors and actuators pervasive onboard automobiles. In the future intelligent transportation system, IVNs are crucial to realize many features of an automobile, including the safety critical features like x-by-wire systems, the intelligent driving features like advanced driving assistance systems and the entertainment features like in-vehicle entertainment systems. All these features involve communications within the vehicle, which are supported by the IVN. When we consider using Ethernet as the backbone network to support new applications with high data rate requirements [1], there are places onboard an automobile where limited space is available for wiring or the Ethernet wires can not reach. As an attractive alternative, PLC uses the existing direct current power lines in an automobile as the communication medium. The complexity and amount of wiring in an au-

tomobile can thus be significantly reduced, which reduces weight and saves cost. The reduction of total wire weight in an automobile also contributes to fuel saving and CO_2 reduction.

HAN provides solutions to communications among various in-home and mobile devices. In the future Internet of Things, in-home multimedia applications and home automation applications will simultaneous run over the HAN. In-home multimedia applications, including video conferencing and in-home gaming, provide both convenience and entertainment to the household residents. Home automation applications, including smart metering and smart controlling, brings us towards a smart home. Over the past few decades, the data rates supported by BB-PLC systems have increased dramatically [5], which makes BB-PLC an attractive solution to HAN. In addition, the access points of BB-PLC, i.e. power outlets, are pervasive in an in-home environment and BB-PLC make use of the existing in-home power line infrastructure, which avoids additional installation costs compared to other solutions to HAN.

We consider using a popular BB-PLC protocol, HomePlug AV (HPAV) [6], to provide solutions to IVN and HAN. Along with supporting multimedia traffic with high data rate transmission requirements [7], the HPAV standard also offers many favourable features like short frame transmissions with robust modulation scheme (referred to as ROBO mode in [6]). Moreover, developed as a subset of HPAV, HomePlug Green PHY (HPGP) [8] supports reliable data transmission among low cost devices with reduced overhead. These are very beneficial to handle the heterogeneous network traffic with different transmission requirements in an IVN or a HAN. Due to the shared nature of power lines as a communication medium, carrier sense multiple access (CSMA) is very efficient as a multiple access scheme under light to medium traffic loads [9]. Therefore, in the remaining part of this thesis, we consider the cases where only CSMA is applied.

However, there are different characteristics and transmission requirements associated with each of the specific application scenarios. Applying the current HPAV protocol without any adaptations will cause some problems detailed in Section 1.2, which makes the deployment BB-PLC in these two application scenarios less attractive. Targeting these problems, this thesis proposes some efficient access control schemes.

1.2 Research Problems

Many research problems exist in each of the two considered application scenarios. In this thesis, we partially address these issues by handling four of these problems, two in each considered application scenario.

1.2.1 Research Problems in IVNs

In an IVN, automobile applications are classified into four classes by the Society of Automobile Engineers. Each class has its own requirements of data rates, latency and reliability. While we can use the ROBO modulation scheme to provide reliable data communication, it is very difficult for an IVN implemented with the current HPAV protocol to meet the stringent quality of service (QoS) requirements of the network traffic involved [1, 10]. In order to make BB-PLC a viable solution, we need to **improve the latency behaviour of different classes of network traffic**.

In an HPAV network, each message is associated with a priority level and a total of four priority levels are supported by the HPAV protocol. We can exploit the prioritization of network traffic to realize the QoS differentiation in an in-vehicle PLC network. However, the HPAV protocol implements the strict priority transmission selection algorithm (TXSA), which means the transmissions of lower priority messages should always yield to those of higher priority messages. The resultant long burst of higher priority messages significantly degrades the QoS of lower priority messages. A new TXSA, which **better deals with the relationship between different priority levels**, needs to be proposed.

1.2.2 Research Problems in HANs

In a HAN, despite the high physical (PHY) layer data rate supported by the HPAV protocol, it remains a challenge to effectively translate this data rate into throughput in the medium access control (MAC) layer. The efficiency of HPAV MAC protocol is largely confined by various kinds of MAC overheads. The CSMA with collision avoidance (CSMA/CA) operation is associated with the lengthy collision recovery. Regardless of this, the HPAV protocol implements CSMA/CA

because collision detection (CD) generally requires in-band full duplexing (IBFD) operations [11, Ch. 5]. Moreover, in order to avoid collisions, each CSMA/CA transmission is associated with a random back-off stage, which further restricts the achieved MAC throughput. We need to reduce these MAC overheads caused by contentions and collisions to **improve the MAC efficiency**.

In order to accommodate heterogeneous network traffic generated by various applications running over PLC HANs, an interface with QoS differentiation is required. The HPAV uses multiple priority levels to prioritize the network traffic. Yet, a specific network traffic prioritization scheme for HANs needs to be proposed. To better manage the network resource utilized by each priority level, in particular, to prevent lower priority starvation, a traffic shaping scheme is required. Thus, we need to **propose an interface with network traffic prioritization and traffic shaping**.

1.3 Summary of Contributions

We can summarize our contributions in this thesis as follows:

- We introduce a Virtual Collision (VC) mechanism as an enhancement to the original HPAV random back-off procedure. The VC mechanism provides better queuing fairness in accordance with the first-in-first-out (FIFO) principle. As a result, the latencies of different network traffic types are effectively reduced, which makes PLC more suitable for IVN uses.

- We propose to combine the strict priority TXSA and Audio Video Bridging (AVB) credit-based shaping (CBS) TXSA as the new TXSA for in-vehicle PLC network. In addition to better dealing with the relationships between the transmissions of different classes of network traffic, safety critical feature of a vehicle is guaranteed with the highest priority.

- Leveraging IBFD capability [12], we propose two schemes, Mutual Preamble Detection (MPD) and Contention-Free Pre-sensing (CFP), to improve MAC efficiency. MPD is the first practical scheme to realize CD in a BB-PLC network while CFP eliminates the superfluous random back-off stages under contention free condition (CFC). Considering the imperfection of IBFD, we analytically show the feasibility of our solutions. These two schemes work well

with each other and achieve over 95% of the optimum MAC efficiency, which can only be attained in the idealized case of no contentions or collisions.

- We provide an interface with network traffic prioritization and traffic shaping to accommodate heterogeneous network traffic involved in a HAN, which is not available in the literature. The network traffic prioritization enables QoS differentiation while the traffic shaping helps support network resource allocation, stream admission control as well as prevents lower priority starvation.

1.4 Outline of the Thesis

The rest of the thesis is organized as follows: In Chapter 2, we provide some background information as well as list some related work. In Chapter 3, we introduce the VC mechanism as well as a new TXSA, as two queuing enhancements for in-vehicle time-sensitive streams, in order to provide timely delivery for different classes of network traffic with consideration of both contention and congestion. We evaluate the effectiveness of our proposed schemes by presenting the simulation results of message delivery latencies under different network settings. In Chapter 4, we explain the efficient access control schemes developed for HAN. We evaluate the effectiveness of our proposed schemes by presenting the simulation results of MAC efficiencies under different network settings. In Chapter 5, we draw conclusions as well as give some suggestions for future work.

Chapter 2

Background

2.1 Development of Power Line Communications

The emergence of PLC technology can be dated back to the late 1800s when first applied to remote meter reading. Since then, PLC technology has continuously evolved [5]. Before the late 1990s, most PLC systems developed fall under ultra-narrowband and low data rate narrowband PLC with a maximum data rate typically lying below a few kbps. Smart grid applications [3] have been one of the main driving forces of PLC systems with higher data rates. Utility companies develop these applications for monitoring, controlling, and maintaining the power grid. Since the late 1990s, the deregulation of telecommunications and energy markets in Europe has fostered the development of BB-PLC systems with a data rate ranging from several Mbps to several hundred Mbps.

Note that the power line medium was not originally designed for data transmission and the power line is actually a very harsh environment for communications [4]. The power line medium is known to be subject to varieties of noise including background noise, synchronous impulse noise, asynchronous impulse noise and aperiodic impulse noise. To address this noise problem, various signal processing techniques have been developed, which are indispensable for the successful development of BB-PLC systems.

Through the years, the data rate supported by BB-PLC systems has increased dramatically. With frequency band extension, IEEE 1901 supports a data rate as high as 500 Mbps [13]. Fur-

ther with multiple-input multiple-output transmission technology, HomePlug AV2 promises a peak PHY data rate up to 1012 Mbps [14].

The high data rates supported by BB-PLC make it an appealing solution to IVN or HAN.

2.2 In-Vehicle Networks and Power Line Communications

The IVN involves communications among different ECUs, sensors and actuators. According to the Society of Automotive Engineers, the number of ECUs in an automobile ranges from 30 for simple cars to approximately 100 for luxury cars. The electronics accounts for 15 percent of total vehicle cost in 2005, climbing from 5 percent in the late 1970s. Today, vehicles are increasingly behaving as an intelligent computing system.[1]

2.2.1 Development of In-Vehicle Networks

At the early stage of contemporary automobile designs, in-vehicle communications are commonly realized through point-to-point wiring between electronic components, resulting in bulky, expensive and complicated harnesses. With increasing scale and complexity, the in-vehicle network grows into a state where volume, weight and reliability becomes a real problem [15, 16]. As a result, a more integral solution is called for and several automobile communication bus protocols have been developed. By connecting a number of the electronic components to the same in-vehicle communication bus, the communication medium can be shared and wiring can thus be saved. Meanwhile, the in-vehicle architecture can be more hierarchical and structural, which also simplifies the automobile designing procedure.

2.2.2 Network Architecture for Future In-Vehicle Networks

Due to the increasing data rate requirements introduced by new applications, e.g., the latest camera-based advanced driver assistance systems, it becomes attractive to use Ethernet as the backbone of next generation in-vehicle networks [1]. However, most of the space of an automobile is occupied by the cabin, which results in limited space available to accommodate wiring. In addition, there are

[1] http://www.nytimes.com/2010/02/05/technology/05electronics.html?_r=0

places where Ethernet wires cannot reach, e.g., where an aftermarket reversing radar is installed. On the other hand, all electronic devices need power supply to function properly. In-vehicle PLC uses the existing DC power line as the communication medium, which significantly reduces the complexity and the amount of wiring in an automobile. This leads to not only savings in the design and manufacturing costs, but more importantly fuel saving and CO_2 reduction. In addition, in-vehicle PLC is extremely beneficial where cabling space is strictly restricted, which is not an uncommon scenario, since in automobile much of the physical space is taken up by the passenger cabin. Therefore, PLC is an attractive supplement to the existing solutions for IVNs.

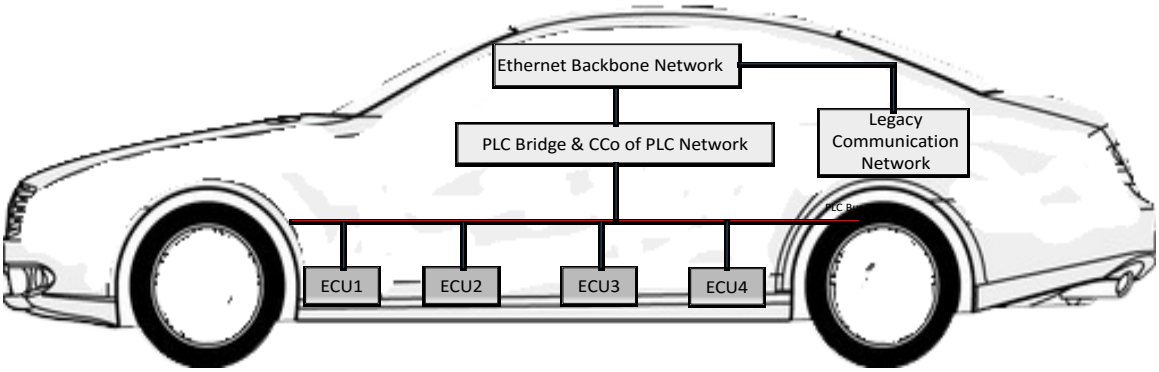

Figure 2.1: An Example of In-Vehicle Network Topology

Fig. 2.1 shows a typical IVN topology. In the figure, ECUs are interconnected to each other through the PLC bus. Messages heading for the Ethernet backbone network are transmitted to the PLC bridge, which forwards arriving packets from the PLC network to the Ethernet backbone and vice versa. The bridge also acts as the central coordinator (CCo) of the PLC network to realize various network management functions. Other legacy networks may coexist with the PLC network.

2.2.3 HPGP Protocol in IVNs

While several protocols exist for off-the-shelf IVNs, most of these protocols, such as Local Interconnect Network and Controller Area Network, are based on the wired communication medium with twisted pairs of wires. None of these protocols can be readily applied to the PLC network because of the unique characteristics of the PLC channel [17].

On the other hand, developed as a subset of HPAV, HPGP [8] is a reliable PLC protocol, which

Table 2.1: In-Vehicle Network Traffic Latency requirements

Traffic Class	Max End-to-End Delay
Control Data	2.5 ms
Safety Data (Video)	45 ms
Infotainment Data	150 ms

is popular due to its low cost and smaller overhead incurred. Thus, we consider HPGP for in-vehicle PLC protocol. However, some modifications are necessary because of the stringent QoS requirements of IVN applications. Antonioli *et al.* have shown [10] that the latency of the current HPGP protocol is too long for many applications, and may have difficulty meeting the requirements of in-vehicle traffic as shown in Table 2.1 [1].

2.2.4 Network Traffic Types

There are several types of network traffic involved in an IVN [18]. We denote all the ECUs including the CCo as network nodes. Each message is sent as one or more data packets. We classify data packets according to their QoS requirements.

Four classes of data packets are considered [19]. Real-time control packets are usually small in size and have low data rate requirements, but they should be delivered with strict time constraints since they are typically generated by safety critical applications, such as drive-by-wire. Data packets generated by other systems, like the comfort system and the infotainment system, are classified into critical application packets, excellent effort packets, and best effort packets. Critical application packets have higher QoS requirements than the excellent effort packets. Best effort packets are sent without any QoS guarantee.

We aim to design efficient access schemes for in-vehicle PLC networks which can meet the latency requirements of all types of network traffic.

2.2.5 Packet Latency

In this thesis, the latency of a packet is measured from the instance when the packet is originated and enters the queuing buffer at the source node to the instance when the source node receives an acknowledgment (ACK) from the destination node indicating that the packet has been success-

fully received. Note that in case of a collision, the data packet is not received at the destination node and the ACK is not returned; thus the packet latency measurement continues and it includes the retransmissions caused by a collision. However, we assume that the IVN traffic is transmitted using a robust modulation scheme (referred to as ROBO mode in [6]); thus we do not consider transmission errors in an IVN and the packet latency measurement does not include the retransmissions caused by transmission errors as we assume that such retransmissions never occur. In such a condition, the packet latency is measured with considerations of collisions and congestions only.

2.2.6 Related Work

Previously, Cano and Malone have carried out simulations [20] and experimental tests [21] on HPAV Protocol, focusing on the network throughput under saturated traffic, rather than network latency. However, saturated traffic is not desired in IVNs because it induces much larger latency. Antonioli *et al.* have made some modifications to the MAC layer of HPGP [10]. However, their work overlooked the buffer queuing delay from upper layers. Sheng *et al.* have proposed a multi-channel MAC protocol for vehicular power line communication systems [22]. By resolving collisions in both the time and frequency domains, the collision overhead can be significantly reduced. However, the robustness of using frequency domain to resolve collisions is questionable.

2.3 Home Area Networks and Power Line Communications

Since the introduction of the 10-Mbps class BB-PLC products using HomePlug 1.0, data rates provided by BB-PLC have increased multi-folds [23]. Current HomePlug AV2 compliant devices use multiple wires available in most in-home wiring installations to achieve multiple-input multiple-output operation, and offer data rates of up to 2 Gbps [7]. The gigabit range of throughput and the widespread availability of access points, i.e., power outlets, makes BB-PLC an attractive solution for a backbone and/or stand-alone communication medium for HANs [5, 24].

Due to the inherent upward and downward compatibility that HPAV provides with other Home-

Plug releases, as well as with IEEE 1901 standard, all solutions we propose can be easily extended to these BB-PLC standards compliant devices as well [25].

2.3.1 Translate PHY Data Rate into MAC Layer

Despite the high data rates obtained at the PHY layer, it remains a challenge to translate this PHY data rate efficiently into MAC throughput. In a CSMA/CA operation, overheads like inter-frame spaces, transmission of priority resolution symbols (PRSs) and transmission of frame control (FC) messages consume additional time. Moreover, CSMA is implemented with CA using a random back-off strategy to prevent collisions. When a collision occurs, a relatively long time is spent on collision recovery [6]. Since no payload data is transferred over the medium during the random back-off or the collision recovery, these MAC overheads caused by contentions and collisions considerably reduce the achieved MAC throughput. Nevertheless, HPAV standard uses CSMA/CA in place of CSMA/CD, since CD requires network nodes to support full-duplex operation [11, Ch. 5].

2.3.2 Improve MAC Efficiency using IBFD

IBFD has recently been successfully applied in a BB-PLC system [12]. The authors proposed a two-step Echo Cancellation (EC) scheme in order to cancel the self-interference (SI) which is a main hurdle in realizing IBFD. The IBFD implementation enables network nodes to sense the medium while simultaneously transmitting data. This inspires us to propose not only a practical CD scheme, similar to CSMA/CD in full-duplex wireless networks, but also to devise an IBFD-based method to eliminate the redundant back-off stages. Although CSMA/CD is also implemented in early Ethernet networks [26, Ch. 6], they are different from BB-PLC in many aspects.

2.3.3 Related Works on CSMA/CD using IBFD

CSMA/CD was considered infeasible in wireless networks due to the inability of network nodes to transmit and receive signals simultaneously in the same band [27]. Pseudo-CSMA/CD procedures, like CSMA with collision notification (CN), were instead proposed as a middle-ground solution

between CSMA/CA and CSMA/CD [27]. However, the introduction of IBFD has propelled feasible CSMA/CD methods to be proposed for wireless networks. The authors in [28, 29] used IBFD to enable the receiver node to continuously transmit acknowledgments as collision-free indicators while receiving the data payload. Such a scheme not only deprives an IBFD system of the bidirectional data payload transmission, but also potentially causes multiple false alarms in conditions of packet errors. Furthermore, it introduces additional power consumption at the destination node for the continuous acknowledgment transmission [30]. Alternative CSMA/CD techniques were proposed for wireless networks in [31, 32] to detect a collision at the transmitter by sensing the medium during transmission without relying on the feedback from the destination node. However, [31, 32] provided analysis of CSMA/CD under the assumption of Rayleigh channel and a fixed self-interference cancellation performance. In contrast, we specify a complete detection and reaction procedure to realize CSMA/CD in BB-PLC networks through the IBFD detection of preamble symbols, and prove the feasibility of our solution by analytically deriving the detection error and false alarm rates under a worst-case BB-PLC line attenuation condition. We use the self-interference cancellation performance reported in the literature [12, 33], which is shown to be dependent on the power line channel attenuation.

2.3.4 An Interface to Support Various HAN Applications

We aim to provide a unified HAN solution that supports both in-home multimedia traffic [34] as well as home automation applications [35]. Many in-home multimedia applications, like audio and video (AV) streaming [35], require high data rate transmissions [7]. On the other hand, home automation applications, which include various smart home applications, such as monitoring and smart controlling of home appliances, usually require in time robust message delivery [36]. An interface to accommodate the heterogeneous network traffic involved is thus required, which to our best knowledge is currently not available in the literature [13].

2.4 An Introduction to HPAV MAC Protocol

In this section, we briefly introduce the HPAV MAC protocol that we aim to refine in this thesis, and also define the MAC layer throughput and efficiency, which we adopt as the metrics to show the performance enhancements of our proposed access control schemes of CFP and MPD.

2.4.1 CSMA/CA Operation

Fig. 2.2 shows the time line of an MAC frame transmission under a standard CSMA/CA operation. In the following, we describe the parts of this operation that are relevant to the schemes we propose.

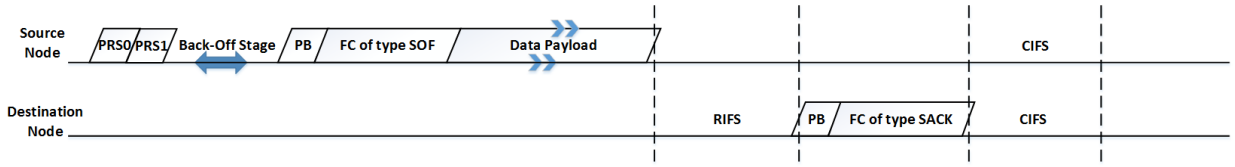

Figure 2.2: MAC frame transmission of HPAV in CSMA/CA mode.

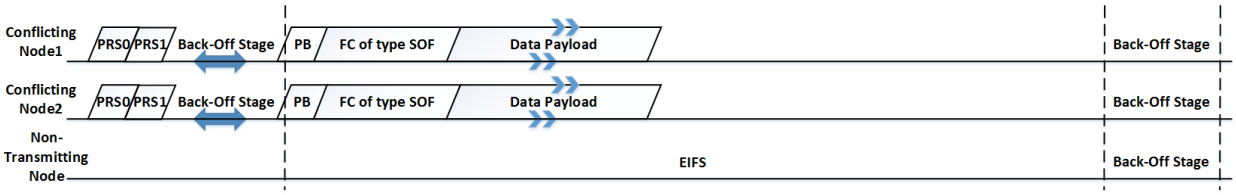

Figure 2.3: Activity on the medium in case of a collision.

Priority Resolution

An MAC frame transmission is initiated with a priority resolution procedure (PRP). The HPAV protocol specifies four priority levels that the network nodes can choose from using two priority bits. The four priority levels are resolved bit-by-bit starting with the slot for PRS_0, and followed by PRS_1, with PRS_0 indicating the most significant bit in the binary representation of the priority level. Each MAC frame is associated with a priority level from 3 (highest) to 0 (lowest). Nodes with the highest priority level in the network win the PRP, which ensures messages of higher priority levels always get transmitted before those of lower priority levels.

Collision Avoidance

Collision avoidance in CSMA/CA is realized through the random back-off mechanism. Nodes winning the PRP proceed to participate in the back-off stage, which consists of a variable number of back-off time slots of equal time interval. At each back-off time slot, a participating node either transmits a preamble or remains silent, while a non-participating node always remains silent during the back-off stage.

When there are no nodes transmitting a preamble in a back-off time slot, all nodes detect this back-off time slot to be idle and nodes participating in the back-off stage decrease their back-off counters (BCs) by one. A participating network node transmits a preamble in a back-off time slot if and only if its BC $= 0$ during that slot. The nodes transmitting a preamble gain access to the channel and then transmit an FC message of type start-of-frame (SOF), followed by the data payload. The other nodes detect the preamble transmission and freeze their BCs until the start of the next back-off stage they participate in.

Apart from BC, the back-off stage also involves three other counters: (a) back-off procedure event counter (BPC), (b) deferral counter (DC), and (c) transmit counter (TC). The TC associates each MAC frame with a life-time. Whenever a network node attempts to transmit an MAC frame, the associated TC will be decreased by one. When TC is decreased to zero, the network node discards the MAC frame. When a network node first enters the back-off stage, it will reset BPC to zero. Each time the BPC is changed or reset, positive integer values of DC and contention window (CW) are set depending on the current BPC value, and BC is randomly set to an integer value uniformly distributed between 0 and CW. Every time a collision is encountered, the BPC is increased by one, and every time a node detects the transmission of MAC frames of the same priority level as its, it decreases DC by one. When DC reaches zero, the network node increases BPC by one.

Collision in the Network

Despite the precautions taken to avoid collisions, CSMA/CA does not guarantee collision-free transmissions, especially with increased number of contending nodes. A collision in the network occurs when multiple nodes simultaneously transmit the preamble signal in a back-off time slot to gain access to the channel. Every node uses a timer called the virtual carrier sense (VCS) timer to determine a collision. At the end of the back-off stage, the timer is set to t_{EIFS}, the time interval of the extended inter-frame space (EIFS), at each network node. A collision is determined at a network node if the node does not receive a selective acknowledgment (SACK) frame before the timer expires. Transmitted by the destination node, an SACK frame is either an ACK frame or an negative acknowledgment (NACK) frame, depending on whether the data payload was successfully decoded. As shown in Fig. 2.2, upon receiving the data payload, the destination node waits for t_{RIFS}, the time interval of the response inter-frame space (RIFS), before transmitting an SACK frame. Note that the VCS timer is also used by the non-transmitting stations to recover from a collision together with all the transmitting stations when the VCS timer expires.

Collision Recovery

Nodes recover from a collision immediately after the EIFS timer expires and start to back-off regardless of the priority level of the transmitting MAC frames. This operation is illustrated in Fig. 2.3. The EIFS has a duration of

$$t_{\mathsf{EIFS}} = 2t_{\mathrm{p}} + 2t_{\mathsf{FC}} + \mathsf{MaxFL} + t_{\mathsf{RIFS}} + t_{\mathsf{CIFS}}, \tag{2.1}$$

where t_{p}, t_{FC} and MaxFL, t_{CIFS} are the time intervals of the preamble, the FC, the maximum time interval of the data payload and the contention inter-frame space (CIFS), respectively. EIFS is therefore lengthy, and renders a collision very costly to recover from.

2.4.2 MAC Throughput and Efficiency

As shown in Fig. 2.2, a data payload is only transmitted during the 'Data Payload' time interval. All other time intervals essentially are overheads that impede the ability of the MAC layer to efficiently translate PHY data rate into MAC throughput. We define the MAC throughput as the rate of successful data packet transmissions, i.e., data rate of packets that are acknowledged by the destination nodes with an ACK.

For N_{pkt} packets successfully transmitted over a time duration T, we define the MAC throughput as

$$S \triangleq \frac{1}{T} \sum_{i=1}^{N_{\text{pkt}}} r_i t_i, \tag{2.2}$$

where r_i and t_i indicate the PHY transmission rate and data payload interval of the ith packet, respectively. For this scenario, the average PHY transmission rate can in turn be expressed as

$$P = \frac{\sum_{i=1}^{N_{\text{pkt}}} r_i t_i}{\sum_{i=1}^{N_{\text{pkt}}} t_i}. \tag{2.3}$$

Thus, we define the ratio of the achieved data rate in the MAC layer to the average performance of PHY layer as the MAC efficiency

$$\eta \triangleq \frac{S}{P} = \frac{1}{T} \sum_{i=1}^{N_{\text{pkt}}} t_i. \tag{2.4}$$

Therefore, to improve S we would typically want to increase the product ηP. However, P is dependent on the nature of the communication channel and advancement of the PLC technology in the PHY layer. In this thesis, we focus on improving η.

The maximum MAC efficiency under CSMA operation can be computed under the condition that a network node continuously transmits frames of maximum length without incurring a transmission error, collision, or backoff[2]. Under such conditions, the maximum MAC efficiency can be

[2]For the sake of simplicity, we ignore the bursting and inverse bursting procedure specified in the HPAV protocol for this computation, without any adverse effects on our proposed solution. Results obtained in this thesis can be easily extended to cases with bursting.

expressed as

$$\eta_{\max} = \frac{\mathsf{MaxFL}}{\mathsf{EIFS} + 2t_{\mathrm{SLOT}}}, \tag{2.5}$$

where $2t_{\mathrm{SLOT}}$ is the time interval for two PRSs. Using the parameters specified in the HPAV standard [6], we obtain $\eta_{\max} = 78.24\%$.

2.4.3 Possible Improvement of MAC Efficiency

In order to enhance practical values of η as close as possible to $\eta_{\max}$, we need to reduce the MAC overheads.

- A collision costs the HPAV network a time interval of EIFS to recover from, which is very lengthy and costly as shown in Fig. 2.3. If we could know beforehand that a collision would occur and avoid it, the MAC efficiency could be considerably improved. We realize this through MPD.

- When a node is the only node transmitting, there will be no contention or collision. The random back-off stage in Fig. 2.2 is superfluous. If we can avoid this superfluous random back-off stage, the MAC efficiency can be further improved. We realize this through CFP.

Chapter 3

Queuing Enhancements for In-Vehicle Time-Sensitive Streams

In this chapter, we propose two queuing enhancements [37] to address two of the problems we encounter when we apply BB-PLC in IVNs. One one hand, the latency performance of the original HPAV protocol is not satisfactory. In this regard, we propose VC as an enhancement to the random back-off procedure specified in the HPGP protocol. VC improves queuing fairness and thus reduces the overall network traffic latency. On the other hand, a new TXSA is needed, which better deals with the relationship between different priority level messages. In this aspect, we combine the AVB CBS TXSA with the strict priority TXSA in order to guarantee the time constraint of real-time control signals and to simultaneously meet the latency requirements of other network traffic.

3.1 Virtual Collision

In the following, we first rewrite the random-back off procedure introduced in Section 2.4.1 in the form of an algorithm. Then we identify its inherent deficiency in the queuing fairness guarantee and introduce the VC mechanism to combat this problem.

3.1.1 Backoff Procedure in HPGP

The random back-off procedure in CSMA specified by the HPGP/HPAV protocol can be divided into three steps, as listed in Algorithm 1. Note that Algorithm 1 is exactly the same procedure as is described in Section 2.4.1. Here we only rewrite it in the form of an algorithm in order to better present our proposed modifications.

Each time the network finishes an MAC frame transmission or the network recovers from a collision, step 1 (back-off status update) is executed. Upon winning the PRP, a network node initializes itself if it has not done so previously. Then in step 1, if BC is zero (in case of initialization or collision) or DC is zero (maximum number of packet deferral reached), the network node resets its BC with an increased BPC. Otherwise DC and BC are decreased since the on-going MAC frame transmission is deferred. The function setCounters() sets DC according to the current BPC and resets BC to be uniformly distributed between zero and the current CW. Then, network nodes winning priority resolution continuously listens to the channel in each back-off time slot and decrease BC by one for each time slot that the communication channel is sensed idle, until BC=0, in which case the node sends out the preamble followed by the SOF FC message and the data payload. The data transmission sets the channel state to busy and the algorithm goes to step 3. In step 3, when an ACK or NACK is received, the transmitting node is reset, or when the timer expires and the ACK or NACK is still not received, the network decides that there is a collision.

3.1.2 Problem Identification

If there is no collision and there is only a single type of network traffic, in order to reduce the maximum latency of packet transmissions, obviously the optimal packet to transmit is the packet that has arrived first and been in queue for the longest time; i.e., FIFO.

In practice, there are multiple types of network traffic interacting with each other. However, the contentions between different types of network traffic are resolved according to the TXSA. Access opportunity allocated by the TXSA to a particular type of network traffic is not affected by the scheduling of packets belong to this traffic type. Thus, for packets belonging to the same traffic

Algorithm 1 Random Backoff Procedure

Step 1 - Backoff Status Update.
Wait for the end of the priority resolution;
if (wonPriorityCheck) **then**
if (!Initialized) **then**
$BC := 0$, $BPC := 0$ and $DC := 0$;
Initialized := true;
end if
if (BC $==0||$DC $==0$) **then**
setCounters(BPC);
BPC$++$;
else
BC$--$, DC$--$;
end if
Listen to the channel;
end if
Step 2 - Random Backoff.
At the beginning of subsequent backoff slot,
if (ChannelBusy) **then**
Goto Step 1;
else if (BC > 0) **then**
BC$--$;
else
Send out message;
end if
Step 3: End of Frame
Before the timer expires,
if (ACKReceived or NACKReceived) **then**
Initialized := false;
Goto Step 1;
end if
When the timer expires,
Goto Step 1;

type, we should still aim for the FIFO queuing. Moreover, retransmissions of collided packets can be considered as another type of network traffic for this discussion.

Without centralized control, Algorithm 1 conforms well to the FIFO queuing principle in most cases. Despite the randomness of the back-off procedure, an early arriving packet on average has undergone more random back-off slots, which means that an early arriving packet has a higher chance to be transmitted. However, Algorithm 1 violates the FIFO queuing principle in the follow-

ing situation.

Assume that there is a collision in the network. For network nodes with non-empty buffers, those involved in the collision will go to a higher contention stage as a penalty and those not involved in the collision will decrease their DC, which is also a penalty with respect to contention. Now, when a data packet is originated at a node with a previously empty buffer, it will initialize the random back-off procedure at the zero contention stage according to Algorithm 1, which yields a smaller contention window size and higher probability of gaining access to the communication medium through contention compared to nodes with non-empty buffers. In the above scenario, the random back-off procedure favours late arrivals of nodes with previously empty buffers, which contradicts the FIFO principle.

3.1.3 Proposed Solution

We propose the VC mechanism, in which Step 1 of the aforementioned random back-off procedure is replaced by that shown in Table 3.1, which differs from the original Step 1 in two respects. Firstly, the buffer of a network node that does not participate in a particular priority level in the PRP is empty with respect to the corresponding type of data packet; BPC is increased each time the random back-off procedure undergoes Step 1 in these nodes. Secondly, the previous BPC value is kept instead of being initialized to zero.

For nodes with non-empty buffers, they follow the exact procedure as specified in Algorithm 1. For nodes with empty buffers, each time a collision occurs, they are considered to be virtually involved in the collision (hence VC) and BPC is increased. As a result, when a data packet is originated, these nodes are penalized to the same degree as network nodes actually involved in the collision, which results in better fairness of buffer queuing with a better conformity to the FIFO queuing principle. Note that the network node with empty buffers will never be over penalized because at each successful transmission, these nodes also assume a virtual successful transmission and reset BPC. Such an improvement in buffer queuing fairness naturally results in a better latency behaviour for the whole network.

Table 3.1: Modified Backoff Status Update

Step 1 - Backoff Status Update.
Wait for the end of the priority resolution;
if (wonPriorityCheck) **then**
if (!Initialized) **then**
$BC := 0$ and $DC := 0$;
Initialized := true;
end if
if (BC $==$ 0||DC $==$ 0) **then**
setCounters(BPC);
BPC$++$;
else
BC$--$, DC$--$;
end if
Listen to the channel;
else
BPC$++$;
end if

3.2 Incorporating AVB Credit Based Shaping

At the beginning of each MAC frame transmission, the network selects the type of data packet to transmit according to the TXSA. We propose to modify the original strict priority TXSA by combining it with the AVB credit-based TXSA. With the proposed new TXSA, the time constraint of real-time control signal can be met and the latency requirements of all other network traffic can also be satisfied.

3.2.1 Existing Transmission Selection Algorithms

IEEE Standard 802.1Q describes the strict priority TXSA [19], whereby lower priority packets are not transmitted until all higher priority packets have been transmitted. During long bursts of high priority traffic, the transmission of lower priority traffic is completely blocked, which significantly increases the latency of lower priority traffic [38]. The AVB credit-based TXSA in IEEE Standard 802.1Qav [39] applies CBS to space out high priority traffic, thus preventing long bursts of high priority traffic.

3.2.2 Proposed Transmission Selection Algorithm

The strict priority TXSA works well to guarantee latency of high priority network traffic. When AVB credit-based TXSA is applied, the latency requirements of all AVB streams can be satisfied under admission control. A combination of these two TXSAs is proposed in this thesis. As a result, the advantages of these two TXSAs can be both realized.

Real-time control signals should be delivered within strict time constraints. Therefore, we give the real-time control signals the highest priority level and whenever there is real-time control signal, other network traffic should yield. Since the real-time control signal is small in packet size and low in data rate requirement, it is not bursty and will not severely block the transmission of lower priority data packets. On the other hand, best effort control signals should yield whenever there is any other network traffic because it is not necessary to guarantee the latency of best effort network traffic. We assign the critical application network traffic as AVB class A stream and the excellent effort network traffic as AVB class B stream. In such a setting, when there is no real-time control signal, AVB class A stream will give way to AVB class B stream if and only if the credit of class A stream is negative and the credit of class B stream is non-negative.

3.2.3 Realization of CBS in HomePlug GP

The CBS is realized through the AVB credit updating procedure. When a class A stream is being sent, the credit of class A stream is decreased with SentSlopeA. Otherwise, the credit of class A stream is increased with IdleSlopeA. The same applies for AVB class B stream with SentSlopeB and IdleSlopeB. IdleSlopeA and IdleSlopeB are exactly the reserved bandwidths for AVB class A stream and class B stream, respectively. SentSlope is the network bandwidth minus the corresponding IdleSlope. For example, we have 10 Mb/s in network bandwidth. We reserve 45 percent network bandwidth for AVB Class A stream; thus IdleSlopeA is 4.5 Mb/s and SentSlopeA is 5.5 Mb/s. In this thesis, we assume an equal bandwidth allocation; i.e., 50% of the network bandwidth are allocated to each type of AVB streams, which also means that we reserve no bandwidth for non AVB streams.

Table 3.2: Simulation Parameters for the IVN

Parameter	Value
Simulation time	30 s
Number of network nodes	10 (including CCo)
Real-time control traffic	50 packets/s/node
Other types traffic	60 packets/s/node
Real-time control packet size	64 byte
Other packet size	128 byte
Data transmission rate	9.8 Mbps
Number of Priority Bits	3
PRS and Backoff Time Slot	5 μs

3.3 Performance Evaluations

We set up a simulation model using OMNet++ to verify the effectiveness of our proposed enhancements. We first specify the simulation parameters and then present and analyze the simulation.

3.3.1 Simulation Configuration

The simulation parameters are presented in Table 3.2. Other parameters are as specified in the HPGP specifications [8]. Different types of data packets arrive from the upper layer of the source node independently according to the Poisson process. All the network nodes are assumed identical and each type of network traffic is originated at each network node independently with the same rate as listed in Table 3.2. The simulation topology is shown in Fig. 3.1. Ten ECUs including the CCo are interconnected with each other through the PLC bus.

3.3.2 Simulation Results and Analysis

The simulation results are presented in Table 3.3, Fig. 3.2 and Fig. 3.3. Table 3.3 shows the maximum latency of all the network nodes. The figures show the maximum latency at various network nodes. Note that the significance of the results is guaranteed by the sufficient simulation time (30s continuous simulation) and multiple independent samples (samples collected from 10 independent and identical network nodes). Admittedly, the maximum latency results become larger as the number of network nodes or the simulation time increases. However, we can apply admission

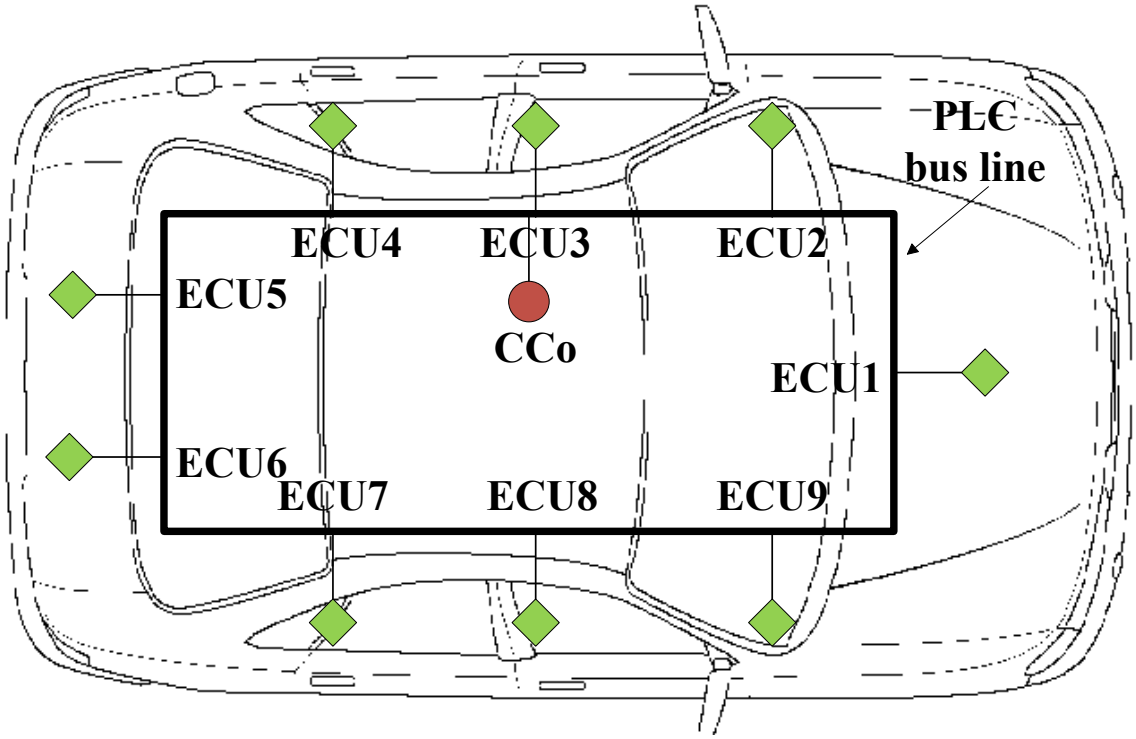

Figure 3.1: Simulation Topology

control to confine the collision rate as the number of network nodes increases. Meanwhile, we can resort to back-up communication systems, should the latency fail to meet the requirements over a longer period of time.

In the results, HPGP corresponds to the latency results obtained by the original HPGP protocol, VC adds the VC mechanism to HPGP, VC+CBS further adds AVB CBS to VC, and IC is the ideal centralized benchmark. In IC, a perfect control channel is assumed over which each network node is able to instantly inform the CCo of its buffer queuing condition, and in each MAC frame access opportunity the CCo selects the network node to transmit according to the FIFO principle.

The results show that when VC is applied, the maximum latency behaviours of all other types of network traffic except best effort are considerably improved, since the improved fairness of buffer queuing causes the network to behave more like a FIFO buffer. From Fig. 3.2 and Fig. 3.3, not only the peak of VC is lower than the peak of HPGP among all the nodes, but also the value of VC for each node is generally lower than the corresponding value of HPGP.

In HPGP and VC, only strict priority TXSA is applied, which is good at securing the latency

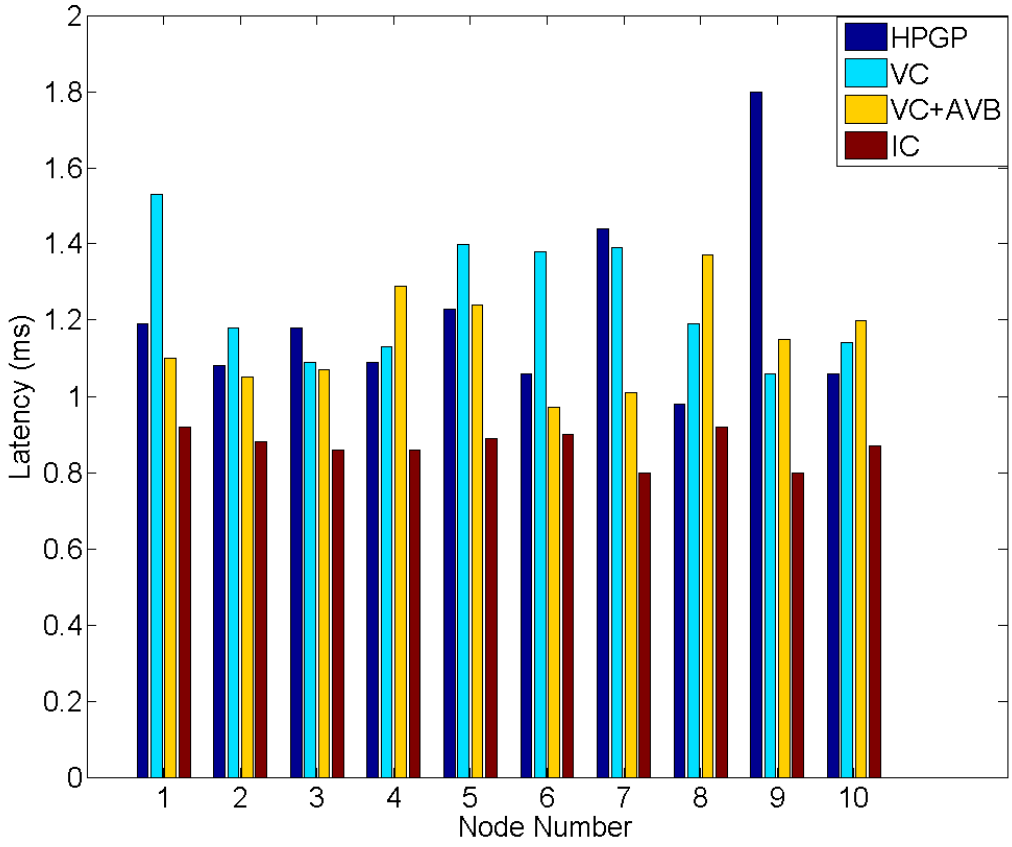

Figure 3.2: Real-Time Control Maximum Latency over 30s Simulations

of higher priority packets, but lower priority packets may be blocked during long bursts of higher priority packets. When AVB CBS is applied, after a burst of AVB stream A, its credit will be negative thus preventing its transmission while the credit of AVB stream B is non-negative. As shown in Table 3.3, when CBS is applied over VC, the maximum latencies of critical application network traffic and excellent effort network traffic are both within 5 ms. Moreover, CBS TXSA is combined with the strict priority TXSA so that the latency of real-time control traffic can be guaranteed.

The results show that the two proposed enhancements, i.e., VC+CBS, effectively lower the latency of real-time control traffic so that it is able to meet more stringent latency requirements, and also keep the latency of critical application and excellent priority traffic within acceptable limits of 5 ms. While the latency of the respective traffic classes is not as low as IC, this is achieved without the overhead of centralized control.

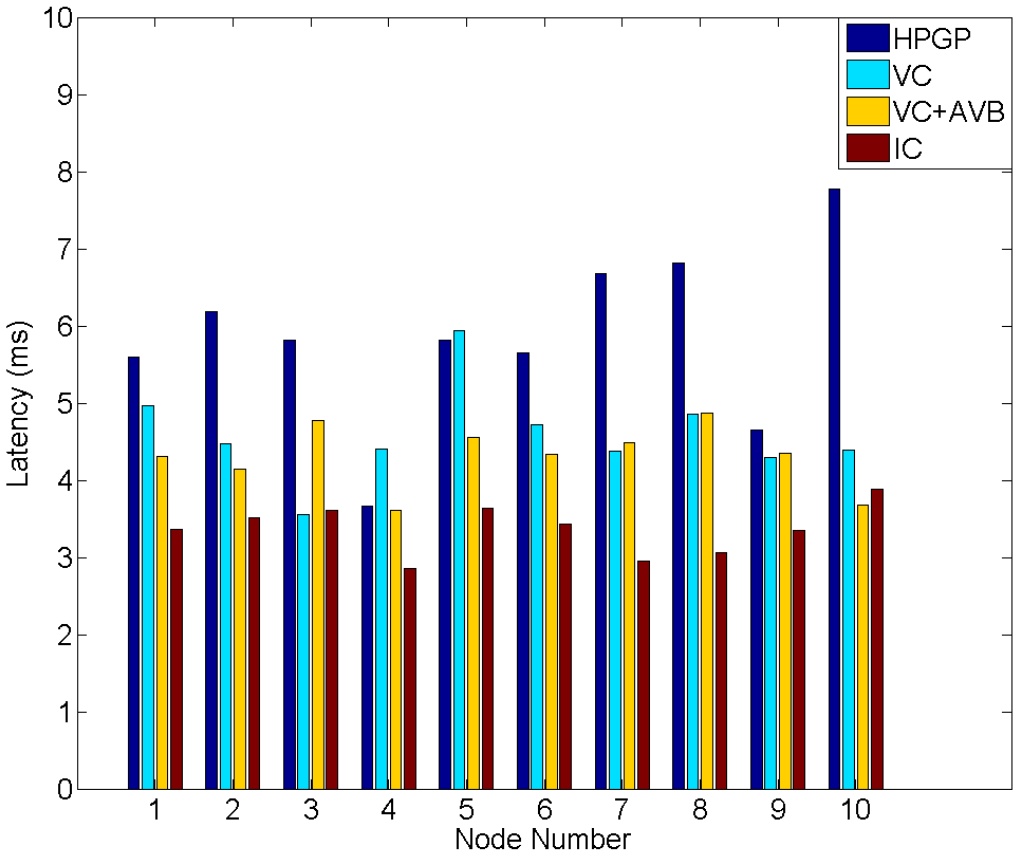

Figure 3.3: Excellent Effort Maximum Latency over 30s Simulations

Table 3.3: Maximum latency of transmitted packets over 30s simulations

	HPGP	VC	VC+CBS	Centralized
Real-Time Control	1.80 ms	1.53 ms	1.37 ms	0.92 ms
Critical Application	3.80 ms	3.07 ms	4.56 ms	2.13 ms
Excellent Effort	7.78 ms	5.94 ms	4.87 ms	3.88 ms
Best Effort	21.09 ms	22.01 ms	22.04 ms	10.86 ms

3.3.3 Discussion on Metrics Used in Evaluations

In this chapter, we want to improve the real-time performance through the adoption of our proposed schemes. Thus, we evaluate the network performance using latency.

Another network metrics to our interest is the throughput. However, we accommodate the network traffic incurred by new applications of high data rate requirements using Ethernet backbone.

The remaining network traffic will not pose much pressure on the PLC network with regard to data throughput. Thus, we do not present network throughput results in our IVN performance evaluations.

3.4 Summary

In this chapter, we have proposed some efficient access control schemes for IVN. We have proposed two enhancements to data packet queuing: the VC mechanism improves the queuing fairness and thus reduces the overall network latency; combining AVB credit-based TXSA with straight priority TXSA minimizes the latency of real-time traffic while satisfying the latency requirements of different traffic classes. We have presented simulation results to demonstrate the effectiveness of our proposal.

Chapter 4

Efficient Access Control Schemes for Home Area Networks

In this chapter, we develop some efficient access control schemes to address two problems that arise when BB-PLC are employed in HANs. On one hand, the PHY data rate is not efficiently translated into throughput in the MAC layer. In this regard, we propose two new techniques that take advantage of IBFD to improve the MAC efficiency. Specifically, we propose CFP to eliminate superfluous random back-off stages and we propose MPD to avoid lengthy collision recovery. On the other hand, an interface to accommodate heterogeneous network traffic generated by various applications running over PLC HAN is not yet available. In this aspect, we propose an interface that uses network traffic prioritization to accommodate their different QoS requirements and traffic shaping to realize centralized bandwidth management and admission control.

4.1 Improving the MAC Efficiency

The format of an HPAV MAC frame transmission in CSMA/CA mode is shown in Fig. 2.2. All the other time intervals except the 'Data Payload' are MAC overheads impeding the MAC efficiency. Note that in case of a collision, the transmitted data payloads corrupt each other and thus all the time intervals shown in Fig. 2.3 are also MAC overheads. With the goal of bringing practical

values of η as close as possible to $\eta_{\max}$, we attempt to reduce the total time duration of these MAC overheads as much as possible. Specifically, we propose CFP to eliminate the redundant back-off stage and MPD to avoid the lengthy collision recovery.

4.1.1 Contention Free Pre-sensing

In this subsection, we propose our first scheme called CFP to detect a CFC during the PRP.

Network Operation with CFP

A CFC is identified by a network node when it does not detect any other network node transmitting with the same or higher priorities during the PRP. To detect a CFC, we equip network nodes with IBFD capability, and allow them to detect the PRS transmitted by other nodes while transmitting a PRS themselves. If a node does not detect any other PRS signal during its PRS transmission, it identifies the channel to be contention free, i.e., detects the presence of a CFC. In case a CFC is detected, as shown in Fig. 4.1, the source node skips the random back-off stage that is traditionally following the PRP, and transmits a preamble signal to gain access to the power line medium immediately after the PRP. Due to this, we observe from Figs. 2.2 and 4.1 that we save a time duration of up to $\mathsf{CW}_{\max} \cdot t_{\mathrm{SLOT}}$, which is otherwise wasted for a redundant back-off, where $\mathsf{CW}_{\max}$ is the maximum contention window size.

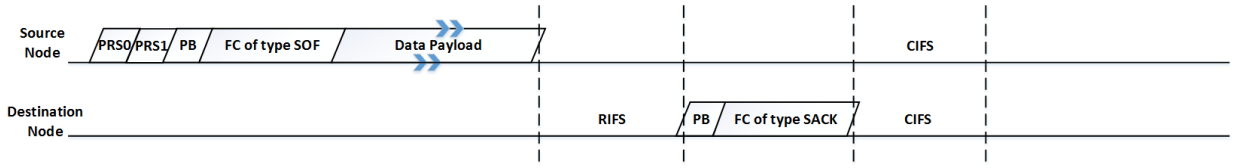

Figure 4.1: MAC frame transmission with CFP when a CFC successfully detected.

Detecting CFC using IBFD CFP

Consider a network of K nodes, where N of those nodes contend to transmit a frame, with priority levels p_n associated with each of the $n = 1, 2, ..., N$ nodes. A CFC occurs when only one of the N nodes transmits a message of the maximum priority level of all transmitting nodes, $\max(p_n)$, with $0 < \max(p_n) \leq p_{\mathrm{std}}$, where $p_{\mathrm{std}} = 2^m - 1$ $(m \in \mathbb{Z}^+)$ is the highest supported priority level of

a message in the operating standard. For example, in the IEEE 1901 and HPAV standards, $m = 2$. In order to provide upward compatibility for future standards that may decide to support a greater number of priority levels to effectively serve traffic of varied nature, we present an analysis of our proposed CFP procedure for general m.

We designate a p_x-CFC to arise when only one network node transmits a message with $\max(p_n) = p_x$. Our CFP scheme is aimed to successfully detect such p_x-CFCs, for all $0 < p_x \leq p_{\text{std}}$. Every priority level p_n can be expressed as

$$p_n = \sum_{i=0}^{m-1} 2^{m-1-i} \chi_i, \tag{4.1}$$

where $\chi_i \in \{0,1\}$ is the binary value of the ith PRS, PRS_i, i.e., $\chi_i = 1$ when a PRS_i is transmitted by the node and $\chi_i = 0$ otherwise. The priority levels are resolved bit-by-bit through the m priority bits from PRS_0 to PRS_{m-1}, with the most significant bit, χ_0, transmitted first as PRS_0. During the PRP, a node of priority p_n transmits the PRS signal in PRS_i $(0 \leq i \leq m-1)$ if and only if $\chi_i = 1$.

Every p_n is associated with a slot position $\bar{j}_n$, for which $\chi_{\bar{j}_n} = 1$ while $\chi_{j_n} = 0$, $\forall j_n > \bar{j}_n$. That is, $\chi_{\bar{j}_n}$ is the least significant 'bit 1' in the binary notation of p_n. With an intention to preserve the legacy PRP and introduce CFP as an add-on feature, we compel the nth network node with priority p_n to perform CFP only at $\mathsf{PRS}_{\bar{j}_n}$, when it has won all previous PRSs. If the node loses the PRP before $\mathsf{PRS}_{\bar{j}_n}$, it resigns from the PRP contention as per the legacy PRP, and therefore does not proceed to perform CFP.

When the node has won in all the previous priority resolution slots, it transmits a PRS at $\mathsf{PRS}_{\bar{j}_n}$, and so will any other node with the same or a higher priority level. Therefore, if the nth node detects another PRS transmitted at $\mathsf{PRS}_{\bar{j}_n}$, it deduces the presence of other node(s) of either the same or a higher priority level. In either case, the nth node deduces a non-CFC. However, if it does not detect any PRS in $\mathsf{PRS}_{\bar{j}_n}$, it deduces the absence of any other node with the same or a higher priority level. In such a CFC, the node skips the following back-off procedure as described in Section 4.1.1. However, it still continues to listen to the medium in the subsequent

PRSs to complete the PRP, to inform other nodes of the on-going transmitting message's priority level in a robust way. By doing so, we also ensure that the CFP procedure does not interfere with the conventional PRP, and is only a supplementary feature introduced to eliminate the redundant back-off time slots under CFC.

The successful detection of a CFC is dependent on the extent of SI cancellation achieved by the IBFD solution. A non-ideal SI cancellation in IBFD could subject CFP to detection failure and false alarms. In the following, we analytically compute the probabilities of detection errors and false alarms using realistic SI cancellation gain values reported in [33].

Detection Error and False Alarm Rates of the CFP

We denote the false alarm and detection error rates of the CFP at a network node as P_{FA} and P_{DE}, respectively. To aid our derivations, we define the following three events at a given network node.

- E_0: The node transmits a PRS.
- E_1: The node detects the presence of at least one PRS signal transmitted by another node in the network.
- E_2: At least one node other than the considered node actually transmits a PRS.

We can now represent $P_{\mathsf{FA}} = P(E_0 \cap (E_1|\bar{E}_2))$, and $P_{\mathsf{DE}} = P(E_0 \cap (\bar{E}_1|E_2))$, where $\bar{E}_n$ represents the non-occurrence of the event E_n.

In order to calculate P_{FA} and P_{DE}, we consider a network with two nodes A and B, with node A continuously transmitting PRSs, while node B either transmits a PRS or remains silent. To determine the detection error and the false alarm rate at node A, we view this scenario as an on-off keying (OOK) transmission, with node B transmitting 'bit 1' when it transmits a PRS, and 'bit 0' when it does not. Here, 'bit 1' corresponds to the PRS signal s_1, whose samples are given by [6]

$$s_1[\ell] = \frac{10^{3/20}}{\sqrt{L}} \sum_{c \in \mathscr{C}} \cos\left(\frac{2\pi \cdot c \cdot \ell}{L} - \psi(c)\right), \quad \ell = 0, 1, ..., L-1, \tag{4.2}$$

where L is the total number of time samples transmitted in the PRS signal, $\mathscr{C}$ is the set of orthogonal frequency division multiplexing (OFDM) sub-carriers used for PRS transmission, and $\psi(c)$ is a sub-carrier specific phase angle [6]. Thus, P_{FA} represents the probability of node A detecting a '1' when a '0' is transmitted by node B, and P_{DE} represents the probability of detecting a '0' when a '1' is transmitted. Considering that the signal is subject to possible phase distortions along the line, we apply non-coherent detection at node A to get [40, Ch. 7]

$$P_{\mathsf{FA}} = \exp\left(-\frac{b_0^2}{2}\right), \tag{4.3}$$

$$P_{\mathsf{DE}} = 1 - \mathscr{Q}\left(\sqrt{2\gamma}, b_0\right), \tag{4.4}$$

where $\mathscr{Q}(\cdot,\cdot)$ is the first-order Marcum-Q function, b_0 is the decision threshold of non-coherent OOK normalized to the root-mean-square noise value, and γ is the signal-to-noise ratio (SNR). The latter is given as

$$\gamma = \frac{E_{\mathrm{b}}}{N_0 + \Psi_{\mathsf{RSI}}}, \tag{4.5}$$

where E_{b} represents the received energy per-bit, N_0 is the average power spectral density (PSD) of the cumulative noise at the receiver of node A, and Ψ_{RSI} is the average residual self-interference (RSI) PSD after non-ideal SI cancellation. For brevity, we define $N_{0,\mathrm{FD}} = N_0 + \Psi_{\mathsf{RSI}}$ as the new effective 'noise floor' under IBFD operation.

To determine realistic values of P_{DE} and P_{FA} in a HAN, we derive an expression for γ in terms of known transmission parameters and channel conditions. The received bit-energy can be written as $E_{\mathrm{b}} = \Phi_{\mathrm{R}} t_{\mathrm{pd}}$, where t_{pd} is the time interval in which CFP is performed, and Φ_{R} is the power of the received signal, which can in turn be written as

$$\Phi_{\mathrm{R}} = \int_{f_1}^{f_2} \Psi_{\mathrm{R}}(f)\mathrm{d}f, \tag{4.6}$$

with $\Psi_{\mathrm{R}}(f)$ being the PSD of the received signal at a frequency f, and f_1 and f_2 are the lower and upper frequency limits of the transmission band, respectively. We further express $\Psi_{\mathrm{R}}(f)$ in

terms of the known transmit PSD, $\Psi_{\mathrm{T}}(f)$, as $\Psi_{\mathrm{R}}(f) = \Psi_{\mathrm{T}}(f) \cdot |H(f)|^2$, where H is the power line channel frequency response between nodes A and B. The maximum transmit PSD is typically regulated to limit the electromagnetic interference caused by BB-PLC [25]. For our analysis, we consider the devices to always transmit signals with maximum PSD $\Psi_{\mathrm{T,max}}$, although newer devices support variable transmit PSDs [14]. Further, it is safe to assume the channel gain to be flat within each sub-carrier, since the HPAV PRS sub-carrier spacing is smaller than the observed channel coherence bandwidth in typical in-home BB-PLC networks [6, 41]. We can therefore re-write (4.6) as

$$\Phi_{\mathrm{R}} = \Psi_{\mathrm{T,max}} \sum_{c \in \mathscr{C}} |H(f_c)|^2 \cdot \Delta f, \tag{4.7}$$

where f_c is the center frequency of the cth OFDM sub-carrier, and Δf is the sub-carrier spacing. Since $N_{0,\mathrm{FD}} = \frac{1}{|\mathscr{C}|} \sum_{c \in \mathscr{C}} N_{0,\mathrm{FD}}(f_c)$, where $N_{0,\mathrm{FD}}(f_c)$ is the effective noise floor of the cth OFDM sub-carrier under IBFD operation, we express (4.5) as

$$\gamma = \Psi_{\mathrm{T,max}} t_{\mathrm{pd}} \Delta f |\mathscr{C}| \frac{\sum_{c \in \mathscr{C}} |H(f_c)|^2}{\sum_{c \in \mathscr{C}} N_{0,\mathrm{FD}}(f_c)}. \tag{4.8}$$

We now determine the optimal value of the threshold b_0 to be used in (4.3) and (4.4). Denoting the overall network node error rate as

$$P_{\mathrm{e}} = P(E_2|E_0) P_{\mathsf{DE}} + P(\bar{E}_2|E_0) P_{\mathsf{FA}}, \tag{4.9}$$

we define the optimal threshold as

$$b_{\mathrm{opt}} \triangleq \arg\min_{b_0} \; P_{\mathrm{e}}. \tag{4.10}$$

In the appendix, we derive the following approximate solution to (4.10),

$$b_{\mathrm{opt}} \approx \sqrt{\frac{(\gamma + \ln \tau)^2 + 4(\gamma + \ln \tau)}{2\gamma}}, \tag{4.11}$$

Table 4.1: PRS SNR under Varying Minimum Channel Gains

$\lvert H_{\min}\rvert^2$ (dB)	$\mathsf{SNR}_{\mathsf{HD}}$ (dB)	SCINR (dB)	$N_{0,\mathrm{FD}}$ (dBm/Hz)	$\gamma_{\min}$ (dB)
-5	65	32	-87	60
-10	60	30	-90	58
-20	50	27	-97	56
-30	40	27	-107	56
-40	30	21	-111	50
-50	20	12	-112	40
-60	10	2	-112	30

where $\tau = \frac{P(\bar{E}_2|E_0)}{P(E_2|E_0)}$. The value of τ depends on the network condition (between idle and heavily loaded).

Since P_{e} is a monotonically decreasing function with respect to γ for optimal threshold b_{opt} [40, Ch. 7], and since $\frac{|H(f_c)|^2}{N_{0,\mathrm{FD}}(f_c)}$ decreases with $|H(f_c)|^2$ [12], we use a flat minimum channel gain, $|H_{\min}|^2$, to obtain an upper bound for the total error, P_{tot}, as

$$P_{\mathrm{tot}} = P_{\mathsf{FA}} + \tau P_{\mathsf{DE}} \tag{4.12}$$

$$\leq 1 - \mathscr{Q}\left(\sqrt{2\gamma_{\min}}, b_{\mathrm{opt}}\right) + \tau \exp\left(-\frac{b_{\mathrm{opt}}^2}{2}\right), \tag{4.13}$$

$$\text{where } \gamma_{\min} = \frac{\Psi_{\mathrm{T,max}}|\mathscr{C}||H_{\min}|^2 \Delta f t_{\mathrm{pd}}}{N_{0,\mathrm{FD}}},$$

and $N_{0,\mathrm{FD}}$ is now the effective IBFD noise floor for a channel gain of $|H_{\min}|^2$.

Using (4.13), we calculate practical upper-bound values of P_{tot} that we expect to encounter when CFP is deployed in in-home networks. In accordance with the HPAV specifications, we set $\Psi_{\mathrm{T,max}} = -50$ dBm/Hz, $\Delta f = 195$ kHz, $|\mathscr{C}| = 153$, and $t_{\mathrm{pd}} = 25.92$ μs [6]. We use an ambient power line noise PSD of $N_0 = -120$ dBm/Hz as the noise floor at the receiver in half-duplex mode. Note that the effective noise floor under IBFD operation is related to N_0 as

$$N_{0,\mathrm{FD}} = N_0 \cdot \frac{\mathsf{SNR}_{\mathsf{HD}}}{\mathsf{SCINR}}, \tag{4.14}$$

where $\mathsf{SNR}_{\mathsf{HD}}$ is the SNR of the signal-of-interest (SOI) in half-duplex mode, and SCINR is the signal-to-canceled-interference-plus-noise-ratio after the SI cancellation [12]. We then use the SI cancellation gain values reported in [12, Table II] to obtain $\gamma_{\min}$ for different minimum channel gains in Table 4.1. From (4.11), we can further calculate b_{opt} for each obtained $\gamma_{\min}$.

As an example, we consider the case where $\tau = 1$ to evaluate P_{DE} and P_{FA}. With $\tau = 1$, (4.11) simplifies to

$$b_{\text{opt}} \approx \sqrt{\frac{\gamma}{2} + 2}. \tag{4.15}$$

With the values computed in Table 4.1 and (4.15), we calculate P_{tot} to be near-zero ($< 10^{-100}$) under various minimum channel gain conditions down to $|H_{\min}|^2 = -60$ dB. From (4.12), we can also use P_{tot} as the individual upper-bound for both P_{FA} and P_{DE}, since $0 \leq P_{\mathsf{FA}}, P_{\mathsf{DE}} \leq 1$. For other τ values, we have similar results and P_{tot}, P_{FA} and P_{DE} are all vanishingly small. This assures us that the deployment of CFP in practical in-home BB-PLC network environments results in virtually no detection errors or false alarms.

4.1.2 Mutual Preamble Detection

We now introduce our second access control enhamcement called MPD, where we use the medium-aware transmission ability provided by the IBFD capability to avoid lengthy collision recovery by predicting a future frame collision. Through MPD, we essentially propose a practical scheme to realize CSMA/CD in BB-PLC networks by detecting the overlapping preamble signals.

Network Operation with MPD

We consider all nodes in the network are equipped with the ability to transmit a preamble and simultaneously sense the power line medium for other possible preamble signal transmissions. In this way, when two or more network nodes transmit a preamble signal at the same back-off time slot and gain access to the power line channel simultaneously, they each predict a future data payload collision by detecting a preamble other than their own. Under such circumstances, we compel these conflicting nodes to transmit another preamble signal subsequently. This acts as a

jamming signal to ensure that all network nodes are made aware of a potential collision. We then let the nodes follow the standard HPAV collision recovery procedure in a guard interval of t_{CIFS}. This operation is illustrated in Fig. 4.2.

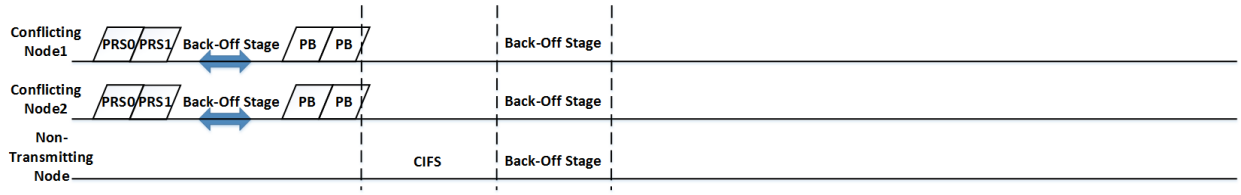

Figure 4.2: Activity on the medium in case of a collision with the deployment of MPD.

We notice that the time interval between the two back-off stages (the back-off stage of the colliding MAC frame and the back-off stage after the collision recovery) is reduced to $2t_{\mathrm{p}} + t_{\mathsf{CIFS}}$ with our MPD scheme, while it is of duration t_{EIFS} in the original HPAV MAC protocol, as shown in Fig. 2.3.

IBFD Preamble Detection

To determine the success of an IBFD preamble detection, consider a BB-PLC network with two nodes, A and B, with node A continuously transmitting preambles slot-by-slot, while in each time slot, node B either transmits a preamble or not. Similar to Section 4.1.1, we view the behavior of node B as a source continuously transmitting information bits using OOK, with the preamble signal being the transmission pulse. In every preamble time slot, node B transmits a bit '1' to send a preamble to node A, and a '0' when it has nothing to transmit. An IBFD enabled node A is able to continuously detect the information bit sent by node B in each time slot. This scenario is similar to the one considered in Section 4.1.1, albeit, the transmission pulse is now a preamble signal, s_2, where

$$s_2[\ell] = \frac{10^{3/20}}{\sqrt{L}} \sum_{c \in \mathscr{C}} \cos\left(\frac{2\pi \cdot c \cdot \ell}{L} + \psi(c)\right), \quad \ell = 0, 1, ..., L-1, \tag{4.16}$$

with the value of L being the same as that for the PRS signal. The preambles also use the same set of OFDM sub-carriers as the PRSs, with the phase shift of each corresponding sub-carrier being the same in magnitude but opposite in sign. Therefore, the P_{FA} and P_{DE} formulations in Section 4.1.1 also apply to the above scenario. This also implies that all the computations in (4.3) to (4.13), as well as the data reported in Table 4.1, are valid for detecting preambles as well. Thus, the detection error rate and the false alarm rate for MPD are also practically zero.

4.1.3 Implementation of CFP and MPD in a BB-PLC Device

Hardware Implementation Costs

The elementary requirement for implementing CFP and MPD in power line networks is to incorporate BB-PLC modems with IBFD capability. Recent works have shown that adding IBFD capability to a BB-PLC device requires minimal changes to the modem chipsets, with only an additional power consumption of about 0.1 W for the active hybrid circuit that is used at the power line-modem interface [33].

Interoperability

Our proposed CFP and MPD schemes are completely inter-operable with half-duplex (HD) devices. For CFP, an IBFD-enabled node can detect a CFC when it is the only node transmitting the highest priority message regardless of whether the other nodes are IBFD-enabled. However, an HD node is unable to detect a CFC. For MPD, when only a part of the network nodes are IBFD-enabled, MPD still offers improvements in η, but with reduced effect compared to the case when all the network nodes are IBFD-enabled. As long as the conflicting nodes are IBFD-enabled, a data payload collision can be successfully predicted and avoided using MPD. However, when an HD node is involved as a conflicting node, the ensuing data payload collision is inevitable, and it takes the network a time interval of EIFS to recover from it.

4.2 An Interface to Accomodate HAN Applications

We aim to provide a unified solution to support various applications running over PLC HANs, which include in-home multimedia applications as well as home automation applications. To accommodate the heterogenous network traffic generated by these applications, in this section, we propose an interface with network traffic prioritization and traffic shaping.

4.2.1 Network Traffic Generated by HAN Applications

We first look into the network traffic generated by various HAN applications.

1. *Home Automation Applications:* Home automation traffic is typically short in duration but frequent in occurrence. It generally consists of data collected by various sensors, like temperature monitoring data, or control commands sent by control units, like turning on/off a device. Due to the large number of sensors, controllers, and actuators in future in-home environments [42], we expect the number of data packets to be also large. These data packets require in-time robust delivery. However, there are also applications like video surveillance that require greater bandwidth. In addition, there is always a constant background information network traffic that only requires a best-effort delivery.

2. *In-home Multimedia Applications:* Multimedia data are generally AV streams that are, for example, generated by video conferencing, in-home gaming, or high-definition AV streaming. These are bursty in nature and have high data throughput requirements [43]. Concurrently, network traffic generated by in-home multimedia applications are also required to be delivered robustly in time. However, multimedia traffic also consists of accompanying control messages that are to be handled similar to home automation traffic, and background information data that only require best-effort delivery.

3. *PLC Network Management Function:* HANs also contain critical network management traffic that requires in-time robust delivery.

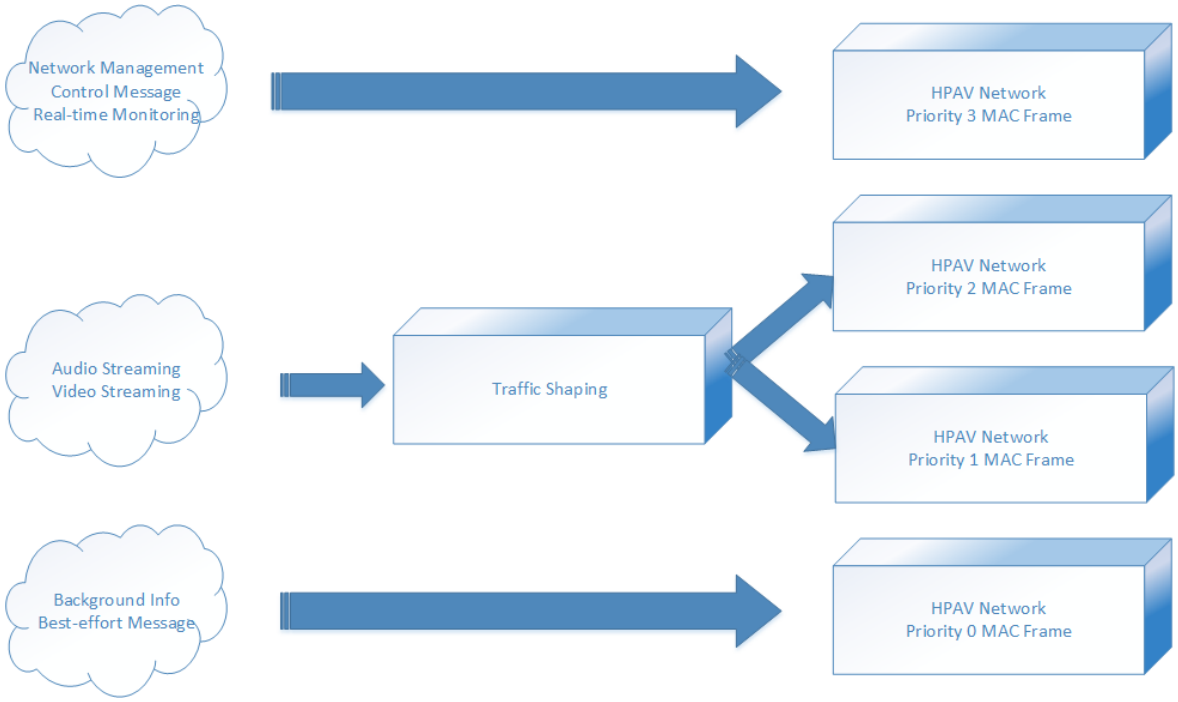

Figure 4.3: Ilustration of Prioritization and Traffic Shaping

4.2.2 Prioritizing HAN Traffic

The heterogeneous network traffic generated by these applications require HANs to provide QoS differentiation function. Since the HPAV protocol supports MAC frame transmissions with different priority levels, we propose a specific network traffic prioritization scheme for the HAN. We assign the highest priority level to network management traffic, control messages, and real-time monitoring data, which we classify as general control message. Next, we assign the next two lower priority levels to multimedia traffic, which mainly includes AV streaming data. Finally, we assign priority 0 to background information traffic flow and all other best-effort network traffic. An illustration of this network traffic prioritization scheme can be found in Fig. 4.3.

Since we prioritize the HAN traffic, we briefly describe the characteristics and requirements of the associated MAC frames.

1. *Priority 3*: General control messages typically require in-time robust delivery. Some of these messages are generated in a cyclic manner while some other are triggered event based. We express the average arrival rates of priority 3 MAC frames at the nth network node as $\lambda_{n,3}$,

which depends on the average message generation rates of general control messages.

2. *Priority 2 and 1*: We reserve these priorities to multimedia traffic. The multimedia content is either stored locally at the source node or is retrieved from external sources (typically the Internet). In either case, the source node pre-fetches multimedia content into the buffer to ensure that there is always some AV streaming data ready to be transmitted beforehand. Such a pre-fetching (also referred to in the literature as buffering or caching) is required at the source node for the smooth delivery of multimedia streams [44–46]. This avoids jitters in the AV playback that could significantly degrade user experience. In order for the efficient playback of the buffered data, as well as to prevent lower priority starvation and to prevent multimedia traffic from using up all the network resource, in Section 4.2.3, we propose the use of traffic shaping as is shown in Fig. 4.3.

3. *Priority 0*: After serving the higher priority traffic, we tune the network nodes to utilize the remaining resources to transmit as many priority 0 MAC frames as possible. In order to fully utilize the network resources, we supply each network with a constant requirement to transmit priority 0 MAC frames.

4.2.3 Traffic Shaping

Several traffic shapers like Poisson traffic shaping (PTS), token-bucket shaping, and credit-based shaping could be implemented in our network [39, 47, 48]. As an example, we incorporate the PTS as our traffic shaping scheme. A Poisson traffic shaper simply pushes the content stored in the buffer into the MAC layer as a Poisson process [48].

The PTS is realized through the CCo of the PLC logical network [7, Ch. 8.5.4.1]. The CCo dynamically allocates $\lambda_{n,i}$ to each of the network nodes through beacon payload messages, where $\lambda_{n,i}$ denotes the arrival rate of the nth network node for the ith priority MAC frame ($i \in \{1,2\}$). Once a node receives this allocation, it pushes the buffered packets of the ith priority level with a random inter-arrival time drawn from an exponential distribution with a mean of $\frac{1}{\lambda_{n,i}}$.

4.2.4 Admission Control

In order to provide each priority level with an appropriate share of the network resource, we implement admission control for the data packets. We denote the average MAC frame intervals at the nth network node as $\mu_{n,i}$ for the ith priority MAC frame ($i \in \{1,2,3\}$). This can be seen in Fig. 2.2 as the duration from the beginning of the PRS_0 to the end of the CIFS.

For a network with N active network nodes, admission control at the CCo ensures that

$$\sum_{n=1}^{N} (\mu_{n,3}\lambda_{n,3} + \mu_{n,2}\lambda_{n,2} + \mu_{n,1}\lambda_{n,1}) = \kappa, \tag{4.17}$$

where $\kappa < 1$. This guarantees the first three priority level messages to be delivered without accumulating at any node. We should also choose a parameter κ way smaller than 1 to account for a fair portion of the network resource to be reserved for collisions, retransmissions as well as best effort message transmissions.

Under scenarios where the relationship of (4.17) cannot be satisfied, switching from CSMA-only mode to a CSMA-plus-TDMA mode is appropriate [13]. For example, when multiple nodes in the network are transmitting high-speed video streams of equal priority levels, it is more suitable to serve them in a round-robin fashion.

4.3 Performance Evaluations

In order to verify the effectiveness of our proposed schemes, we simulate the in-home PLC network and evaluate their performance in three different network settings using a discrete event simulator, OMNeT++ [49].

4.3.1 Simulation Configuration

The simulation network topology is shown in Fig. 4.4. Several network nodes, including the CCo, are interconnected to each other through the power line medium in a star configuration. Out of these, only a set of $\mathcal{N}$ nodes are active with data to transmit. In our simulations, we assume

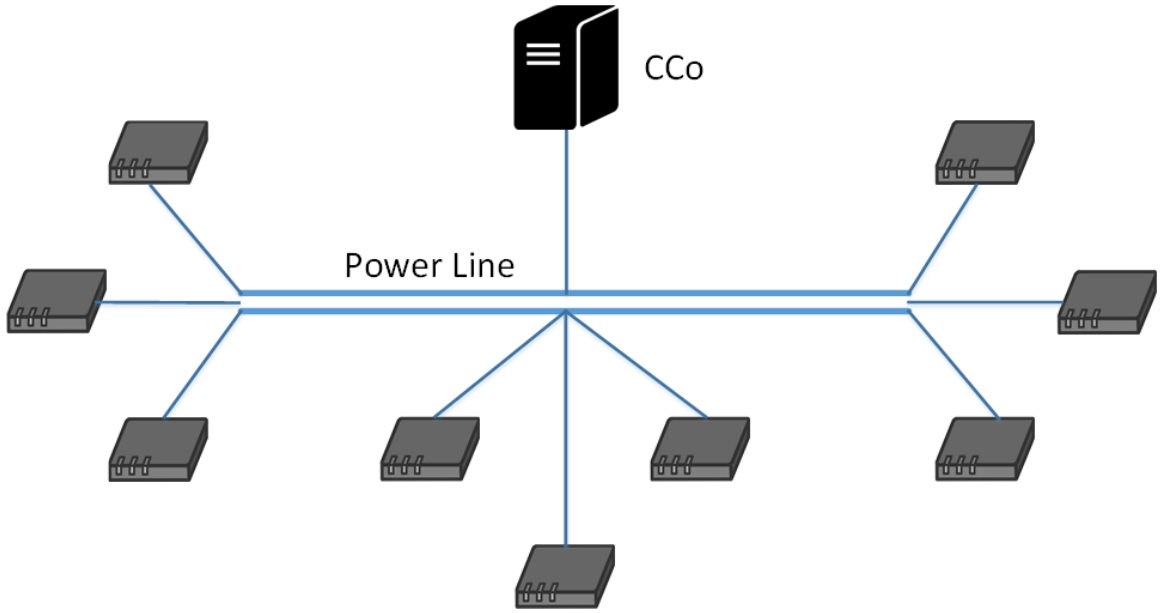

Figure 4.4: Network Simulation Topology

Table 4.2: Simulation Parameters for the HAN

Parameter	Value
Simulation Time, T_S	30 s
t_{CIFS}	100 μs
PRS and Back-off slot time, t_{SLOT}	35.84 μs
t_p	35.84 μs
t_{FC}	133.92 μs
MaxFL	2341.12 μs
t_{RIFS}	140 μs
t_{EIFS}	2920.64 μs

an identical time interval of the data payload, t_{FL}, regardless of its priority level. The simulation parameters are listed in Table 4.2, and are based on the HPAV specifications [6]. The significance of the simulation results is guaranteed by the sufficient simulation time, T_S, where the resultant MAC efficiency of each simulation run is the average performance of several thousands of MAC frame transmissions.

By denoting the total number of transmitted MAC frames with successful acknowledgments as n_{ACK}, we compute the MAC efficiency, η, at the end of our simulation runs as

$$\eta = \frac{n_{ACK} t_{FL}}{T_S}, \tag{4.18}$$

where T_S is the total simulation time (see Table 4.2).

We assume that the physical layer uses a robust transmission mode (referred to as ROBO mode in [25]) to transmit control sequences, while we consider the multimedia streams with inherent data redundancy to be error tolerant. Therefore, for simplicity, we do not consider transmission errors as well as the associated retransmissions in our simulation [50, 51]. In such conditions, n_{ACK} is simply equal to the total number of frames transmitted without encountering collisions.

4.3.2 Performance of CFP with Single Node Flooding

For our first result, we use the following network setting to test the effectiveness of the CFP scheme. We set $|\mathscr{N}| = 1$ by letting the CCo be the only active network node that continuously transmits priority-3 MAC frames to all the other network nodes without channel idling. Under such a scenario, our proposed MPD scheme has no effect as no contention or collision occurs with this setting. The impact of varying t_{FL} on the achieved MAC efficiency with and without CFP is shown in Fig. 4.5.

Since the network experiences no collision or idle time intervals, the power line medium is kept busy by continuously transmitting MAC frames shown in Fig. 2.2. Under such conditions, the MAC efficiency can also be represented as

$$\eta = \frac{t_{\mathsf{FL}}}{(t_{\mathsf{EIFS}} - \mathsf{MaxFL}) + t_{\mathsf{FL}} + (2 + \mathbb{E}[n_{\text{BF}}])t_{\text{SLOT}}}, \tag{4.19}$$

where $\mathbb{E}[n_{\text{BF}}]$ is the expected number of back-off time slots. Using the HPAV protocol without CFP, the contention remains at the base stage of 0 as no node other than the CCo transmits packets, and hence the transmission of these packets encounters no collisions or deferral [6]. As a result, every time the CCo transmits a MAC frame, the BC is randomized to an integer value uniformly distributed between 0 and CW_{min}, where CW_{min} is the smallest contention window size (7, as specified in the HPAV protocol). Therefore, $\mathbb{E}[n_{\text{BF}}] = \frac{7}{2} = 3.5$. However, with our CFP deployed, the CCo detects a CFC at every frame transmission, since there are no other contending nodes. Thus, the redundant back-offs are avoided at the CCo. This results in $\mathbb{E}[n_{\text{BF}}] = 0$, thereby increasing η.

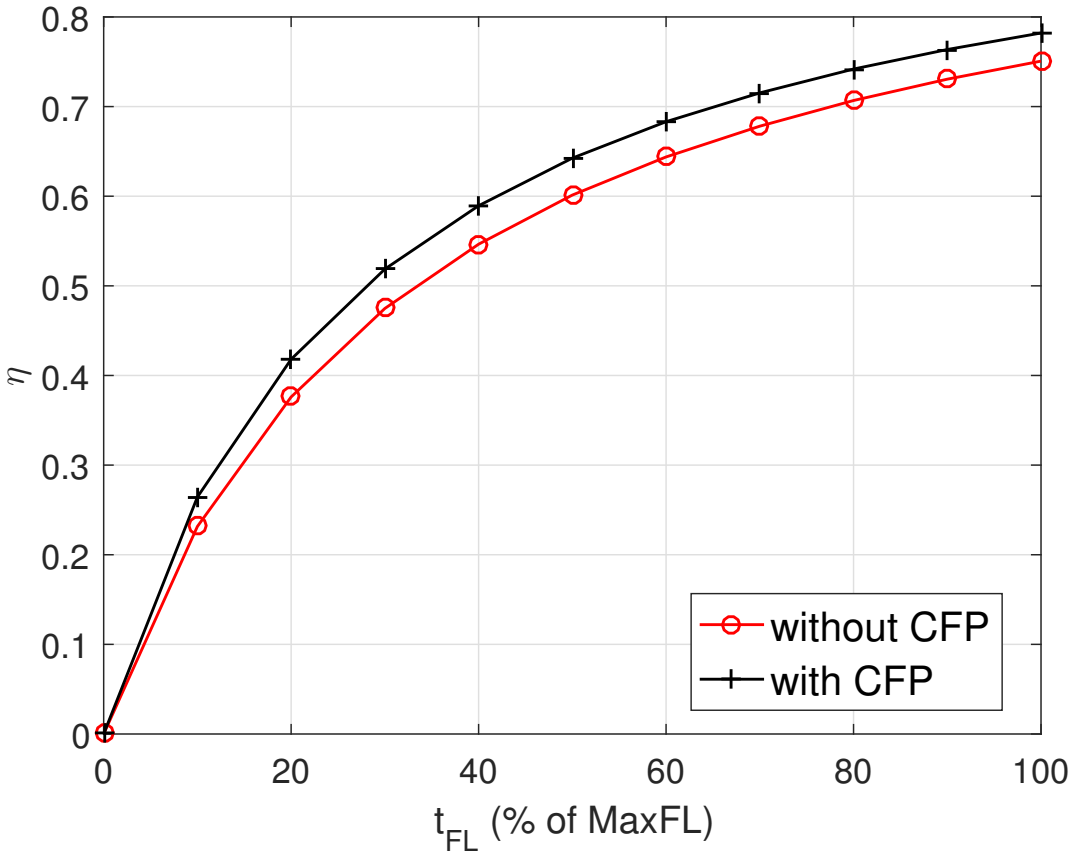

Figure 4.5: MAC efficiency as a function of t_{FL} under single node flooding.

Furthermore, when we set $t_{\mathsf{FL}} = \mathsf{MaxFL}$ for our CFP deployment, we observe $\eta = 78.21\%$, which is close to the theoretical maximum of $\eta_{\max} = 78.24\%$ (from (2.5)). The slight difference can be attributed to the bootstrapping process of our simulations, as well as the last frame in our simulations not being able to finish its transmission within the total simulation time. When these simulation non-idealities are accounted for, the achieved MAC efficiency reaches the theoretical maximum with $t_{\mathsf{FL}} = \mathsf{MaxFL}$.

4.3.3 Performance Evaluation with Multiple Active Nodes

To evaluate the network performance with multiple active nodes, we enable $1 < |\mathscr{N}| \leq 25$. We form two sub-settings where we fix $|\mathscr{N}| = 10$ and vary t_{FL} in the first case, while we fix $t_{\mathsf{FL}} = \mathsf{MaxFL}$ and vary $|\mathscr{N}|$ in the second.

Network Resource Allocation

We calculate the average MAC frame interval at the nth network node in our simulations as

$$\mu_{n,i} = (t_{\mathsf{EIFS}} - \mathsf{MaxFL}) + t_{\mathsf{FL}} + (2 + \mathbb{E}[n_{\mathrm{BF}}]_{n,i}) t_{\mathrm{SLOT}}, \tag{4.20}$$

for the ith priority MAC frame, where $\mathbb{E}[n_{\mathrm{BF}}]_{n,i}$ represents expected number of back-off time slots at the nth network node for the ith priority data packet. Since the number of back-off time slots is hard to predict, we approximate $\mu_{n,i}$ as

$$\mu_{n,i} \approx \mu = (t_{\mathsf{EIFS}} - \mathsf{MaxFL}) + t_{\mathsf{FL}} + 2t_{\mathrm{SLOT}}. \tag{4.21}$$

Thus, by considering the above approximation, the admission control in our simulations can be expressed by re-writing (4.17) as

$$\mu \sum_{n=1}^{|\mathscr{N}|} (\lambda_{n,3} + \lambda_{n,2} + \lambda_{n,1}) = \kappa. \tag{4.22}$$

To account for the back-off time slots we ignored in our approximation of $\mu_{n,i}$, we choose a small $\kappa = 0.65$. By setting $\sum_{n=1}^{|\mathscr{N}|} \lambda_{n,i} = \frac{\kappa_i}{\mu}$, we allocate a certain portion of network resource to the ith priority network traffic, which for simplicity, we further allot equally to all $|\mathscr{N}|$ network nodes. Thus, we have $\lambda_{n,i} = \frac{1}{|\mathscr{N}|}\frac{\kappa_i}{\mu}$, $\forall n \in \mathscr{N}$ and $i \in \{1,2\}$. For general control messages, we assume an equal event rate at each network node as $\lambda_{n,3} = \frac{1}{|\mathscr{N}|}\frac{\kappa_3}{\mu}$, $\forall n \in \mathscr{N}$. In our simulations, we assume $\kappa_3 = 0.25$, and $\kappa_2 = \kappa_1 = 0.2$.

Performance Evaluations with Varying t_{FL}

We first simulate the network with varying t_{FL} and fix $|\mathscr{N}| = 10$. The variation of the MAC efficiency with varying t_{FL} is shown in Fig. 4.6. The curves essentially resemble those in single node flooding, but with reduced η, because of contentions and collisions. However, all our proposed schemes improve the MAC efficiency compared to the standard HPAV protocol.

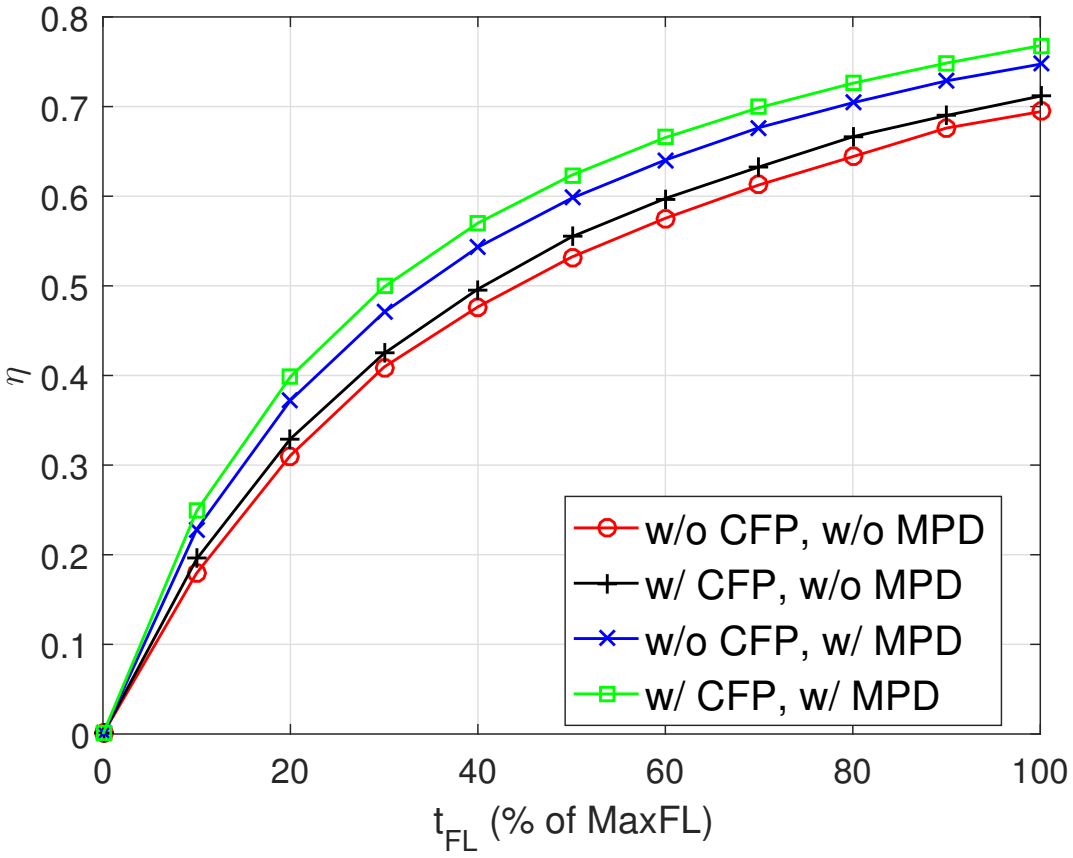

Figure 4.6: MAC efficiency as a function of t_{FL}.

We observe that simultaneous deployment of CFP and MPD yields an $\eta = 76.80\%$, which achieves 98.16% of the optimal MAC efficiency, $\eta_{\max} = 78.24\%$. At the same time, we notice that a conventional HPAV protocol without CFP and MPD only manages to provide $\eta = 69.43\%$.

Performance Evaluations with Varying Number of Active Nodes

For our final result, we simulate the network with varying $|\mathcal{N}|$ and a fixed $t_{\mathsf{FL}} = \mathsf{MaxFL}$. The simulation results of this subsetting are shown in Fig. 4.7. We observe that without our MPD scheme, η decreases as the number of active network nodes increases due to the increased collision rate as well as the lengthy collision recovery time. However, we achieve a stable η across different number of nodes with MPD since our proposed MPD scheme virtually achieves CD. With our MPD scheme, the potential collisions can be successfully detected and avoided, which brings the cost of

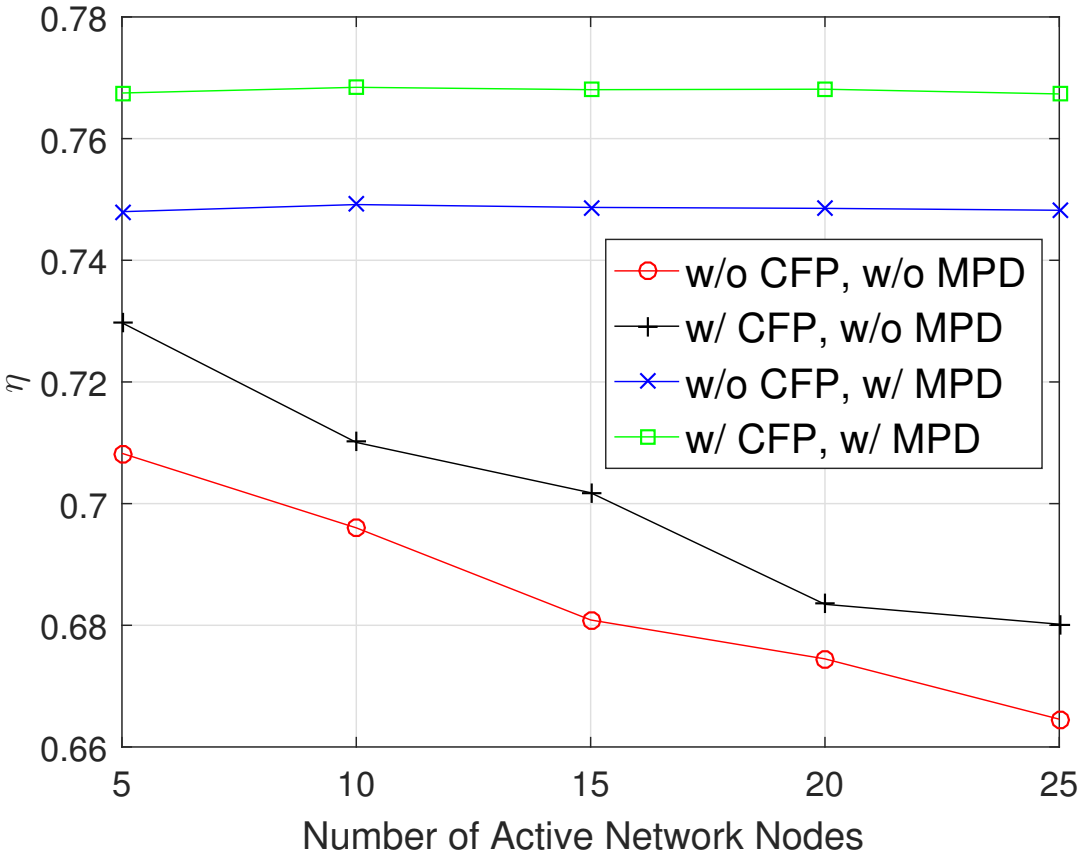

Figure 4.7: MAC efficiency as a function of the number of active nodes.

a potential collision to the minimum. Because of this, as the number of network nodes increases, although the collision rate is increased, we do not observe a degradation of MAC efficiency when our MPD scheme is applied. We further observe that although the use of CFP without MPD does not provide a stable η across varying nodes, it still manages to improve η from that obtained with the original HPAV protocol, as a result of redundant back-off times being eliminated under CFCs. We also observe that we obtain the best η, both in terms of absolute value and stability across increasing nodes, using both our proposed schemes of CFP and MPD.

4.3.4 Discussion on Metrics Used in Evaluations

In this chapter, we aim to improve the MAC efficiency through the adoption of our proposed schemes. Thus, we evaluate the network performance under various conditions using MAC effi-

ciency.

Another network metrics to our interest is the latency of network traffic with non-zero priority level. However, we use admission control to ensure that messages of first three priority levels can be emptied from time to time. The probability of a message with non-zero priority level staying in the network goes exponentially small as the staying time increases. Thus, we do not present latency data in our HAN performance evaluations.

4.4 Summary

In this chapter, we have proposed some efficient access control schemes for BB-PLC in HAN. In order to efficiently translate PHY data rate onto the MAC throughput, we have leveraged IBFD to propose two novel schemes, CFP and MPD. CFP eliminates the redundant back-off stages while MPD avoids the lengthy collision recovery. To accommodate heterogeneous network traffic generated by various applications running over PLC HAN, we have proposed an interface with network traffic prioritization and traffic shaping. We have presented simulation results showing under single network node flooding and maximal MAC frame size conditions, theoretical optimal MAC efficiency can be achieved. We have shown that under various conditions, CFP works well with MPD to considerably increase the MAC efficiency close to optimal value while each scheme standing alone can also provide MAC efficiency improvements over the original HPAV protocol.

Chapter 5

Conclusions

5.1 Summary

In this thesis, we have proposed some efficient access control schemes for IVNs and HANs. In each of the two considered application scenarios, on one hand we have made some refinements to the original MAC protocols to better support the QoS requirements of different network traffic, while on the other hand, we have developed some upper layer specifications to better interface the involved applications.

In Chapter 3, we have explained the details of our proposed efficient access control schemes for IVNs. Through network simulations we have shown that the introduced VC mechanism effectively reduces the latency of different classes of network traffic involved. The proposed TXSA combining strict priority TXSA and AVB CBS TXSA better deals with the relationship between transmissions of different classes of network traffic so that the latency requirements of different classes of network traffic are decently satisfied.

In Chapter 4, we have explained the details of our proposed efficient access control schemes for HANs. Through theoretical and numerical evaluations we have shown our proposed CFP and MPD work well together to considerably increase the MAC efficiency. The PHY data rate are better translated into the throughput in MAC layer. We have also developed an interface to accommodate heterogenous network traffic generated by various applications running over PLC HAN.

We have adopted a comprehensive model in Chapter 3. While such a model is more implicative of what can be achieved in a real scenario, it prevents us from a thorough theoretical analysis, which is more viable under a simplistic model. As a result, the reasoning in this chapter is more heuristic than analytical and the evaluations following is more empirical than theoretical. To improve this, we can first derive analytical results using a simplified model and then discuss implications of these results in a real scenario.

It is noticed that the MAC protocol of a BB-PLC network much resembles that of a wireless network. In particular, CSMA is implemented as the main operation mode in both of the MAC protocols. Access control schemes developed for wireless networks can give us a lot of inspirations when we study related topics in BB-PLC networks. With some adaptions, some schemes developed for wireless networks can be implemented in a BB-PLC network to further improve the network performance.

5.2 Future Directions

For potential extensions of the current work, we suggest to reconsider our proposed schemes in a multi-hop network environment. This also brings about the hidden terminal/exposed terminal problem in which case some enhanced schemes are required to reduce the lengthy collision recovery time or to avoid the superfluous random back-off stage. For example, it is possible that two network nodes both transmit a preamble and each detects no preambles transmitted by other network nodes because of hidden terminals. The original HPAV protocol implements request-to-send/clear-to-send (RTS/CTS) mechanism to overcome this issue. We may also use it in an FD BB-PLC network. However, we expect a more efficient realization using IBFD by overlapping (partially) the transmission of RTS and CTS.

Furthermore, the MAC efficiency can be further improved by monitoring network statistics and dynamically choosing optimum CW. For example, we can implement adaptive schemes with a threshold to vary the size of CW according to the estimated network load.

Bibliography

[1] S. Tuohy, M. Glavin, C. Hughes, E. Jones, M. Trivedi, and L. Kilmartin, "Intra-vehicle networks: A review," *IEEE Transactions on Intelligent Transportation Systems*, vol. 16, no. 2, pp. 534–545, 2015. → pages 1, 3, 7, 9

[2] J.-P. Javaudin, M. Bellec, D. Varoutas, and V. Suraci, "OMEGA ICT project: Towards convergent gigabit home networks," in *IEEE International Symposium on Personal, Indoor and Mobile Radio Communications (PIMRC), Cannes, France*, pp. 1–5, September 2008. → pages 1

[3] S. Galli, A. Scaglione, and Z. Wang, "For the grid and through the grid: The role of power line communications in the smart grid," *Proceedings of the IEEE*, vol. 99, no. 6, pp. 998–1027, 2011. → pages 1, 6

[4] A. Majumder and J. Caffery, "Power line communications," *IEEE Potentials*, vol. 23, no. 4, pp. 4–8, 2004. → pages 1, 6

[5] L. Lampe, A. Tonello, and T. Swart, "Introduction," in *Power Line Communications: Principles, Standards and Applications from Multimedia to Smart Grid* (L. Lampe, A. Tonello, and T. Swart, eds.), ch. 1, pp. 1 – 7, John Wiley and Sons Ltd, 2016. → pages 2, 6, 10

[6] "HomePlug AV specification," *HomePlug Powerline Alliance*, 2007. → pages 2, 10, 11, 17, 32, 33, 34, 35, 43, 44

[7] S. Galli, H. Latchman, V. Oksman, G. Prasad, and L. Yonge, "Multimedia PLC systems," in *Power Line Communications: Principles, Standards and Applications from Multimedia to Smart Grid* (L. Lampe, A. Tonello, and T. Swart, eds.), ch. 8, pp. 475 – 511, John Wiley and Sons Ltd, 2016. → pages 2, 10, 12, 41

[8] H. A. Latchman, S. Katar, L. W. Yonge, and S. Gavette, "HomePlug Green PHY," *Homeplug AV and IEEE 1901: A Handbook for PLC Designers and Users*, pp. 302–311, 2013. → pages 2, 8, 24

[9] N. Pavlidou, A. H. Vinck, J. Yazdani, and B. Honary, "Power line communications: state of the art and future trends," *IEEE Communications Magazine*, vol. 41, no. 4, pp. 34–40, 2003. → pages 2

[10] R. P. Antonioli, M. Roff, Z. Sheng, J. Liu, and V. C. M. Leung, "A real-time MAC protocol for in-vehicle power line communications based on HomePlug GP," in *IEEE Vehicular Technology Conference (VTC Spring), Glasgow, Scotland*, pp. 1–5, May 2015. → pages 3, 9, 10

[11] H. Hrasnica, A. Haidine, and R. Lehnert, *Broadband Powerline Communications: Network Design*. John Wiley and Sons Ltd, 2005. → pages 4, 11

[12] G. Prasad, L. Lampe, and S. Shekhar, "Enhancing transmission efficiency of broadband PLC systems with in-band full duplexing," in *IEEE International Symposium on Power Line Communications and Its Applications (ISPLC), Bottrop, Germany*, March 2016. → pages 4, 11, 12, 35, 36

[13] IEEE Standards Association, "IEEE standard for broadband over power line networks: Medium access control and physical layer specifications," *IEEE Std 1901*, pp. 1–1586, 2010. → pages 6, 12, 42

[14] L. Yonge, J. Abad, K. Afkhamie, L. Guerrieri, S. Katar, H. Lioe, P. Pagani, R. Riva, D. M.

Schneider, and A. Schwager, "An overview of the homeplug AV2 technology," *Journal of Electrical and Computer Engineering*, vol. 2013, 2013. → pages 7, 34

[15] S. Poledna, W. Ettlmayr, and M. Novak, "Communication bus for automotive applications," in *IEEE European Solid-State Circuits Conference (ESSCIRC), Villach, Austria*, pp. 482–485, September 2001. → pages 7

[16] G. Leen, D. Heffernan, and A. Dunne, "Digital networks in the automotive vehicle," *Computing and Control Engineering Journal*, vol. 10, no. 6, pp. 257 – 66, 1999. → pages 7

[17] N. Taherinejad, R. Rosales, L. Lampe, and S. Mirabbasi, "Channel characterization for power line communication in a hybrid electric vehicle," in *IEEE International Symposium on Power Line Communications and Its Applications (ISPLC), Beijing, China*, pp. 328–333, March 2012. → pages 8

[18] G. Alderisi, A. Caltabiano, G. Vasta, G. Iannizzotto, T. Steinbach, and L. L. Bello, "Simulative assessments of IEEE 802.1 Ethernet AVB and time-triggered Ethernet for advanced driver assistance systems and in-car infotainment," in *IEEE Vehicular Networking Conference (VNC), Seoul, Korea*, pp. 187–194, November 2012. → pages 9

[19] IEEE Standards Association, "IEEE standard for local and metropolitan area networks virtual bridged local area networks," *IEEE Std 802.1Q-2005 (Incorporates IEEE Std 802.1Q1998, IEEE Std 802.1u-2001, IEEE Std 802.1v-2001, and IEEE Std 802.1s-2002)*, pp. 1–285, 2006. → pages 9, 22

[20] C. Cano and D. Malone, "Performance evaluation of the priority resolution scheme in PLC networks," in *IEEE International Symposium on Power Line Communications and its Applications (ISPLC), Glasgow, Scotland*, pp. 290–295, March 2014. → pages 10

[21] C. Cano and D. Malone, "When priority resolution goes way too far: An experimental evaluation in PLC networks," in *IEEE International Conference on Communications (ICC), London, U.K.*, pp. 952–957, June 2015. → pages 10

[22] Z. Sheng, A. Kenarsari-Anhari, N. Taherinejad, and V. C. M. Leung, "A multichannel medium access control protocol for vehicular power line communication systems," *IEEE Transactions on Vehicular Technology*, vol. 65, no. 2, pp. 542–554, 2016. → pages 10

[23] "HomePlug 1.0 specification," *HomePlug Powerline Alliance*, 2001. → pages 10

[24] S. Nowak, F.-M. Schaefer, M. Brzozowski, R. Kraemer, and R. Kays, "Towards a convergent digital home network infrastructure," *IEEE Transactions on Consumer Electronics*, vol. 57, no. 4, pp. 1695–1703, 2011. → pages 10

[25] H. A. Latchman, S. Katar, L. Yonge, and S. Gavette, *Homeplug AV and IEEE 1901: A Handbook for PLC Designers and Users*. Wiley-IEEE Press, 2013. → pages 11, 34, 44

[26] A. Leon-Garcia and I. Widjaja, *Communication Networks*. McGraw-Hill Inc., 2003. → pages 11

[27] S. Sen, R. R. Choudhury, and S. Nelakuditi, "CSMA/CN: Carrier sense multiple access with collision notification," *IEEE/ACM Transactions on Networking*, vol. 20, no. 2, pp. 544–556, 2012. → pages 11, 12

[28] T. Vermeulen, F. Rosas, M. Verhelst, and S. Pollin, "Performance analysis of in-band full duplex collision and interference detection in dense networks," in *IEEE Annual Consumer Communications & Networking Conference (CCNC), Las Vegas, NV*, pp. 595–601, January 2016. → pages 12

[29] Y.-S. Choi and H. Shirani-Mehr, "Simultaneous transmission and reception: Algorithm, design and system level performance," *IEEE Transactions on Wireless Communications*, vol. 12, no. 12, pp. 5992–6010, 2013. → pages 12

[30] T. Vermeulen and S. Pollin, "Energy-delay analysis of full duplex wireless communication for sensor networks," in *IEEE Global Communications Conference (GLOBECOM), Austin, TX*, pp. 455–460, December 2014. → pages 12

[31] Y. Liao, K. Bian, L. Song, and Z. Han, "Full-duplex MAC protocol design and analysis," *IEEE Communications Letters*, vol. 19, no. 7, pp. 1185–1188, 2015. → pages 12

[32] L. Song, Y. Liao, K. Bian, L. Song, and Z. Han, "Cross-layer protocol design for CSMA/CD in full-duplex WiFi networks," *IEEE Communications Letters*, vol. 20, no. 4, pp. 792–795, 2016. → pages 12

[33] G. Prasad, L. Lampe, and S. Shekhar, "In-band full duplex broadband power line communications," *IEEE Transactions on Communications*, vol. 64, no. 9, pp. 3915 – 3931, 2016. → pages 12, 32, 38

[34] C. Cano, A. Pittolo, D. Malone, L. Lampe, A. M. Tonello, and A. Dabak, "State-of-the-art in power line communications: From the applications to the medium," *IEEE Journal on Selected Areas in Communications*, vol. 34, no. 7, pp. 1935 – 1952, 2016. → pages 12

[35] Y.-J. Lin, H. A. Latchman, M. Lee, and S. Katar, "A power line communication network infrastructure for the smart home," *IEEE Wireless Communications*, vol. 9, no. 6, pp. 104–111, 2002. → pages 12

[36] G. Hallak and G. Bumiller, "PLC for home and industry automation," in *Power Line Communications: Principles, Standards and Applications from Multimedia to Smart Grid* (L. Lampe, A. Tonello, and T. Swart, eds.), ch. 7, pp. 449 – 472, John Wiley and Sons Ltd, 2016. → pages 12

[37] Y. Huo, Q. Zheng, Z. Sheng, and V. C. M. Leung, "Queuing enhancements for in-vehicle time-sensitive streams using power line communications," in *IEEE/CIC International Conference on Communications in China (ICCC), Shenzhen, China*, pp. 1–6, November 2015. → pages 18

[38] M. D. Johas Teener, A. N. Fredette, C. Boiger, P. Klein, C. Gunther, D. Olsen, and K. Stanton, "Heterogeneous networks for audio and video: Using IEEE 802.1 audio video bridging," *Proceedings of the IEEE*, vol. 101, no. 11, pp. 2339–2354, 2013. → pages 22

[39] IEEE Standards Association, "IEEE standard for local and metropolitan area networks - virtual bridged local area networks amendment 12: Forwarding and queuing enhancements for time-sensitive streams," *IEEE Std 802.1Qav-2009 (Amendment to IEEE Std 802.1Q-2005)*, Jan. 2009. → pages 22, 41

[40] M. Schwartz, W. R. Bennett, and S. Stein, *Communication Systems and Techniques*. John Wiley & Sons, 1995. → pages 33, 35, 60

[41] F. J. Canete, J. Cortés, L. Díez, and J. T. Entrambasaguas, "A channel model proposal for indoor power line communications," *IEEE Communications Magazine*, vol. 49, no. 12, pp. 166–174, 2011. → pages 34

[42] F. Xia, L. T. Yang, L. Wang, and A. Vinel, "Internet of things," *International Journal of Communication Systems*, vol. 25, no. 9, p. 1101, 2012. → pages 39

[43] Z. Sahinoglu and S. Tekinay, "On multimedia networks: Self-similar traffic and network performance," *IEEE Communications Magazine*, vol. 37, no. 1, pp. 48–52, 1999. → pages 39

[44] L. Golab and M. T. Özsu, "Issues in data stream management," *ACM Sigmod Record*, vol. 32, no. 2, pp. 5–14, 2003. → pages 41

[45] S. A. Saberali, H. E. Saffar, L. Lampe, and I. Blake, "Adaptive delivery in caching networks," *IEEE Communications Letters*, vol. 20, pp. 1405 – 1408, July 2016. → pages

[46] R. Rejaie, H. Yu, M. Handley, and D. Estrin, "Multimedia proxy caching mechanism for quality adaptive streaming applications in the Internet," in *Annual Joint Conference of the IEEE Computer and Communications Societies (INFOCOM), Tel Aviv, Israel*, vol. 2, pp. 980–989, March 2000. → pages 41

[47] F. Gomez-Cuba, R. Asorey-Cacheda, and F. J. Gonzalez-Castano, "Smart grid last-mile

communications model and its application to the study of leased broadband wired-access," *IEEE Transactions on Smart Grid*, vol. 4, no. 1, pp. 5–12, 2013. → pages 41

[48] F. P. Kelly, "Networks of queues," *Advances in Applied Probability*, pp. 416–432, 1976. → pages 41

[49] A. Varga, "OMNeT++," in *Modeling and Tools for Network Simulation*, pp. 35–59, Springer, 2010. → pages 42

[50] G. Bianchi, "Performance analysis of the IEEE 802.11 distributed coordination function," *IEEE Journal on selected areas in communications*, vol. 18, no. 3, pp. 535–547, 2000. → pages 44

[51] M. Y. Chung, M.-H. Jung, T.-J. Lee, and Y. Lee, "Performance analysis of HomePlug 1.0 MAC with CSMA/CA," *IEEE Journal on Selected Areas in Communications*, vol. 24, no. 7, pp. 1411–1420, 2006. → pages 44

Appendix

Optimal Detection Threshold

In this appendix, we provide a closed-form expression for the optimum detection threshold, b_{opt}, by solving (4.10). We start with (4.9), and divide both sides by $P(E_2|E_0)$ to get

$$P_\tau = \frac{P_e}{P(E_2|E_0)} = P_{\mathsf{DE}} + \tau P_{\mathsf{FA}}, \tag{5.1}$$

where $\tau = \frac{P(\bar{E}_2|E_0)}{P(E_2|E_0)}$. Since $P(E_2|E_0)$ is a constant for a given network operation, minimizing (5.1) also solves (4.10). Therefore, b_{opt} is the b_0 that solves

$$\frac{\partial P_\tau}{\partial b_0} = 0. \tag{5.2}$$

We first individually find the partial derivatives of both the components of P_τ using (4.3) and (4.4) to get

$$\frac{\partial P_{\mathsf{FA}}}{\partial b_0} = -b_0 \exp\left(-\frac{b_0^2}{2}\right) \tag{5.3}$$

$$\begin{aligned}\frac{\partial P_{\mathsf{DE}}}{\partial b_0} &= \frac{\partial}{\partial b_0}\left(1 - \int_{b_0}^{\infty} x \exp\left(-\frac{x^2+2\gamma}{2}\right) I_0\left(x\sqrt{2\gamma}\right) \mathrm{d}x\right) \\ &= \exp\left(-\frac{2\gamma+b_0^2}{2}\right) I_0\left(b_0\sqrt{2\gamma}\right) b_0,\end{aligned} \tag{5.4}$$

where $I_n(\cdot)$ is the nth-order modified Bessel function of the first kind. By using (5.1)-(5.4), we get

$$\exp(-\gamma) I_0\left(b_{\text{opt}}\sqrt{2\gamma}\right) = \tau. \tag{5.5}$$

Next, we find a closed-form approximation for the transcendental equation of (5.5). To this end, we use the proven result that $b = \sqrt{2+\frac{\gamma}{2}}$ provides an excellent analytic approximation to the solution of $\exp(-\gamma) I_0\left(b\sqrt{2\gamma}\right) = 1$ [40, Eqns. 7-4-13, 7-4-14, Fig. 7-4-3]. Thus, we have

$$\begin{aligned} \exp(\gamma) &\approx I_0\left(\sqrt{\gamma(\gamma+4)}\right) \\ \implies I_0\left(b_{\text{opt}}\sqrt{2\gamma}\right) &\approx \exp\left(\sqrt{2b_{\text{opt}}^2\gamma+4}-2\right). \end{aligned} \tag{5.6}$$

Using (5.6) in (5.5), and simplifying with some simple manipulations gives us the closed-form expression for b_{opt} as

$$b_{\text{opt}} \approx \sqrt{\frac{(\gamma+\ln\tau)^2+4(\gamma+\ln\tau)}{2\gamma}}. \tag{5.7}$$